Dr. Yuh-Lang Lin
Physics/AST 885-05 (Orographic Precipitating Systems)
(http://mesolab.ncat.edu)
NC A&T State University

Lecture Note 15 Mesoscale Instabilities

(Based on Ch. 7 of Mesoscale Dynamics (Lin 2007))

7. Mesoscale Instabilities

Chapter 15 Mesoscale Instabilities

- Observational, theoretical and numerical studies have found that instabilities play important roles in numerous mesoscale phenomena, such as
  squall lines, rain bands, mesoscale convective complexes, mesoscale cyclogenesis, clear air turbulence, billow clouds, heavy orographic precipitating systems, etc.
- Thus, a fundamental understanding of the instabilities occurring at mesoscale and those that influence mesoscale circulations is essential to comprehend these phenomena.
- For example, the momentum and/or potential energy associated with the airflow might be transferred into perturbation kinetic energy through instabilities, which may then disturb the flow or help release latent heating, dramatically disturbing the airflow.
- As discussed in Chapter 1, mesoscale instabilities may serve as one type of energy generation mechanism for mesoscale circulations and weather systems.
- Although instabilities associated with the mean wind velocity or thermal structure of the atmosphere are a rich energy source of atmospheric disturbances, the maximum growth rates of most atmospheric instabilities are either on the large scale, such as ***baroclinic and barotropic instabilities***, or on the microscale, such as ***Kelvin-Helmholtz and static (gravitational) instabilities***.
- ***Symmetric instability*** appears to cover the mesoscale range in the sense that the projected horizontal scale of the slantwise circulation of the unstable mode is often in the mesoscale range.
- Differences between moist and dry convection.
  - In a dry atmosphere, convection includes both unstable updrafts and downdrafts and turbulent eddies, such as the Ralyleigh-Be'nard convection (e.g. Chandrasekar 1961) triggered by the thermal instability between two horizontal plates heated from below.
  - Normally, , *moist convection* in the atmosphere behaves quite differently from dry convection has and the mesoscale cellular convection shown in Fig. 7.1, and is characterized by (Emanuel and Raymond 1984):

- (1) strong, compact, turbulent, unstable, upward motion,
- (2) weak, compensated, laminar, stable downward motion (over a wide area of the surroundings), and
- (3) inertia-gravity waves generated outside and which propagate away from the convective region.

- However, the differences described above may be due to the spatial distribution of the forcing.
  - For example, Figure 7.1 show an example of a mesoscale cellular convection occurred over the Atlantic Ocean observed over the Atlantic Ocean off the southeast coast of the United States on February 19, 2002, as viewed by satellite Terra.

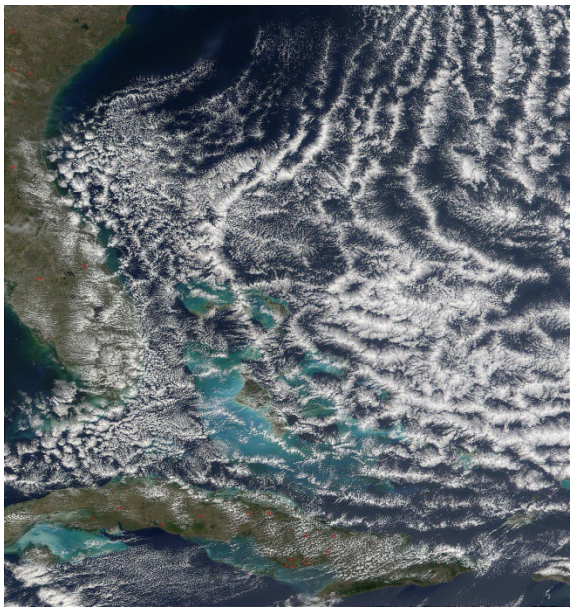

Fig. 7.1: Open cell cloud formation observed over the Atlantic Ocean off the southeast coast of the United States on February 19, 2002, as viewed by satellite Terra. This type of clouds is an atmospheric manifestation of Ralyleigh-Bénard convection is known as mesoscale cellular convection. It normally forms as the cold air passes over the warmer ocean waters. Notice the hexagonal open cells produced in the cloud-topped boundary layer and the convective clouds at the vertices of the hexagonal cells. (From Visible Earth, NASA)

- This type of clouds is an atmospheric manifestation of Rayleigh-Be′nard convection in the atmosphere. It normally forms as the cold air passes over the warmer ocean waters. Notice the hexagonal open cells produced in the cloud-topped boundary layer and the convective clouds at the vertices of the hexagonal cells.

- The open cells have downward motion and clear skies at the center of the cells. Notice the hexagonal open cells produced in the cloud-topped boundary layer and the convective clouds at the vertices of the hexagonal cells.

7.1 Wave Energy Transfer Through Instabilities

- The energy transfer among different forms, such as potential energy and kinetic energy, and through different hydrodynamic instabilities may be understood by examining the linear energy equation.

- The governing equations for a small-amplitude, inviscid, Boussinesq atmosphere on a planetary *f*-plane can be combined into a single equation for the vertical velocity, as derived in Chapter 3,

$$\begin{aligned}&\frac{D}{Dt}\{\frac{D^2}{Dt^2}\nabla^2 w' + f^2 w'_{zz} - (U_{zz}\frac{D}{Dt} + fV_{zz})w'_x - (V_{zz}\frac{D}{Dt} - fU_{zz})w'_y + N^2\nabla_H^2 w' \\ &\quad + 2f(U_z w'_{yz} - V_z w'_{xz})\} + 2fU_z V_z(w'_{xx} - w'_{yy}) + 2f(V_z^2 - U_z^2)w'_{xy} \\ &\quad - 2f^2(U_z w'_{xz} + V_z w'_{yz}) = \frac{g}{c_p T_o}\frac{D}{Dt}\nabla_H^2 q'.\end{aligned} \tag{7.1.1}$$

- As also mentioned in earlier chapters, this equation represents a mesoscale atmospheric system which may contain the following generation mechanisms of:
  (a) pure and inertia-gravity waves,
  (b) static instability,
  (c) conditional instability,
  (d) potential (convective) instability,
  (e) Kelvin-Helmholtz instability,
  (f) symmetric instability,
  (g) inertial instability, (h) baroclinic instability, and
  (i) wave-CISK (conditional instability of the second kind).

- The energy transfer equation for the above system that has no north-south (meridional) basic state wind component ($V = 0$), but includes the meridionally sheared zonal flow ($U_y \neq 0$) can be derived

$$\left(\frac{\partial}{\partial t} + U\frac{\partial}{\partial x}\right)E + \rho_o u'w'U_z + \rho_o u'v'U_y - \left(\frac{\rho_o g f}{N^2\theta_o}\right)v'\theta'U_z + \nabla\cdot(p'v') = \left(\frac{\rho_o g^2}{c_p T_o N^2\theta_o}\right)\theta' q' \tag{7.1.2}$$

where

$$E = \frac{\rho_o}{2}\left[\left(u'^2 + v'^2 + w'^2\right) + \left(\frac{g}{N\theta_o}\right)^2\theta'^2\right], \tag{7.1.3}$$

is the ***total perturbation energy***.

The ***total perturbation energy*** consists of the ***perturbation kinetic energy*** and the ***perturbation potential energy***, which are represented by the first and second terms inside the square bracket, respectively.

Taking the ***horizontal integration*** of Eq. (7.1.2) over a single wavelength for a periodic disturbance or from -∞ to +∞ for a localized disturbance in both *x* and *y* directions gives

$$\frac{\partial\overline{E}}{\partial t} = -\rho_o(\overline{uw})U_z - \rho_o(\overline{uv})U_y + \left(\frac{\rho_o g f}{N^2\theta_o}\right)(\overline{v\theta})U_z - \frac{\partial}{\partial z}(\overline{pw}) + \left(\frac{\rho_o g^2}{c_p T_o N^2\theta_o}\right)(\overline{\theta q})$$

(7.1.4)

➢ Now taking the ***vertical integration*** of the above equation from $z = 0$ to the top of the physical domain or the domain of a finite-area numerical model, $z = z_T$, in which the physical phenomena are investigated or simulated, yields

$$\frac{\partial E_T}{\partial t} = -\rho_o \int_0^{z_T} \overline{uw}\, U_z dz - \rho_o \int_0^{z_T} \overline{uv}\, U_y dz + \left(\frac{\rho_o g f}{N^2 \theta_o}\right) \int_0^{z_T} \overline{v\theta}\, U_z dz$$

(1) (2) (3) (4)

$$- \overline{pw}(z_T) + \overline{pw}(z=0) + \left(\frac{\rho_o g^2}{c_p T_o N^2 \theta_o}\right) \int_0^{z_T} \overline{\theta q}\, dz.$$

(5) (6) (7)

(7.1.5)

where E_T is the domain-integrated total perturbation energy E.

- Term 1: the local rate of change in the total perturbation energy in the system.
- Term 2: the vertical momentum flux transfer between the kinetic energy of the basic current and the perturbation wave energy.
    - When shear instability occurs, the energy is transferred from the basic state shear flow to the perturbation, which results a net loss of kinetic energy of the basic state. In order to show the phase relationship, we may define a *perturbation streamfunction* ψ in a two-dimensional (*x, z*) flow as

$$u = \frac{\partial \psi}{\partial z}; \quad w = -\frac{\partial \psi}{\partial x} \tag{7.1.6}$$

    - Note that the above relationships satisfy the incompressible continuity equation. With this definition, uwU_z can be written as

$$uwU_z = -\left[\frac{\partial \psi}{\partial x} / \frac{\partial \psi}{\partial z}\right]\left(\frac{\partial \psi}{\partial z}\right)^2 U_z = \left[\frac{\partial z}{\partial x}\right]_\psi \left(\frac{\partial \psi}{\partial z}\right)^2 U_z, \tag{7.1.7}$$

since $(\partial\psi/\partial x)dx + (\partial\psi/\partial z)dz = d\psi = 0$ on a constant streamline line ψ.

This in turn implies that when there exists shear instability (i.e. term 1 > 1) if $U_z > 0$, we have on average over the vertical plane

$$\left[\frac{\partial z}{\partial x}\right]_{\psi} < 0. \qquad (7.1.8)$$

- Therefore, the growing wave in an adiabatic stably stratified flow must have a phase tilt in an *opposite direction of the shear vector*, i.e., an *upshear phase tilt*. This also implies that the updraft has an upshear tilt since it is out of phase with the stream function by a factor of $\pi/2$. This phase relationship is sketched in Fig. 7.2.

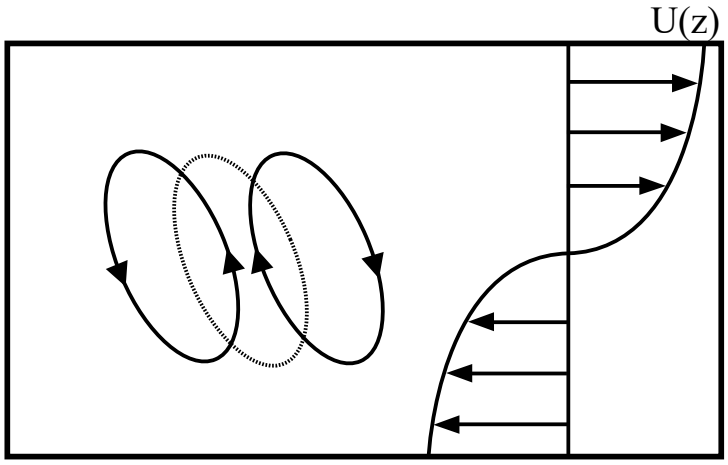

Fig. 7.2: A sketch of the basic wind profile and the upshear tilt of the perturbation streamfunctions (solid) and updraft (dashed) associated with an unstable growing gravity wave in a stably stratified flow. The perturbation wave energy is converted from the basic flow shear. (From Lin and Chun, 1993)

- Term 3: the horizontal momentum flux transfer between the kinetic energy of the basic state shear and the perturbation wave energy. The energy transfer to horizontal momentum occurs when there exists *inertial instability*.

The argument for horizontal phase tilt is similar to the above argument for shear instability.

- Term 4: the energy exchange between the basic state vertical shear and the perturbation heat flux. The basic state vertical shear is supported by the baroclinicity (horizontal temperature gradient) through thermal wind balance.

  Under this situation, available potential energy is stored in the system, which is transferred to perturbation kinetic energy when there exists baroclinic instability.

  This argument is used to explain why the trough tilts westward with height during the midlatitude cyclogenesis.
- Term 5: the forcing from the upper boundary condition.
- Term 6: the forcing from the lower boundary.
- Term 7: the contribution from diabatic source or sink to total perturbation energy.

7.2 Integral Theorems of Stratified Flow

7.2.1 Governing equations

Consider the following inviscid, nonrotating, Boussinesq fluid system with all the nonlinear and inhomogeneous terms lumped into source terms on the right side of the governing equations,

$$\frac{\partial u'}{\partial t}+U\frac{\partial u'}{\partial x}+U_z w'+\frac{1}{\rho_o}\frac{\partial p'}{\partial x}=F_1, \tag{7.2.1}$$

$$\frac{\partial v'}{\partial t}+U\frac{\partial v'}{\partial x}+\frac{1}{\rho_o}\frac{\partial p'}{\partial y}=F_2, \tag{7.2.2}$$

$$\frac{\partial w'}{\partial t}+U\frac{\partial w'}{\partial x}-g\frac{\theta'}{\theta_o}+\frac{1}{\rho_o}\frac{\partial p'}{\partial z}=F_3\,, \tag{7.2.3}$$

$$\frac{\partial u'}{\partial x}+\frac{\partial v'}{\partial y}+\frac{\partial w'}{\partial z}=0\,, \tag{7.2.4}$$

$$\frac{\partial \theta'}{\partial t}+U\frac{\partial \theta'}{\partial x}+\frac{N^2\theta_o}{g}w'=H\,, \tag{7.2.5}$$

where

$$F_1=-\frac{\partial(u'u')}{\partial x}-\frac{\partial(u'v')}{\partial y}-\frac{\partial(u'w')}{\partial z}\,, \tag{7.2.6}$$

$$F_2=-\frac{\partial(v'u')}{\partial x}-\frac{\partial(v'v')}{\partial y}-\frac{\partial(v'w')}{\partial z}\,, \tag{7.2.7}$$

$$F_3=-\frac{\partial(w'u')}{\partial x}-\frac{\partial(w'v')}{\partial y}-\frac{\partial(w'w')}{\partial z}\,, \tag{7.2.8}$$

$$H=\dot{Q}-\frac{g}{\theta_o}\left[\frac{\partial(u'\theta')}{\partial x}+\frac{\partial(v'\theta')}{\partial y}+\frac{\partial(w'\theta')}{\partial z}\right]. \tag{7.2.9}$$

$F=(F_1,F_2,F_3)$ the perturbation *Reynolds stress*,

$\dot{Q}$ the diabatic heating, and

H the *effective heating*, which is composed by the diabatic heating and *turbulent heat fluxes*.

- Considering a 2D flow and taking the normal mode approach by assuming

$$\phi=\hat{\phi}\,e^{ik(x-ct)}\,. \tag{7.2.10}$$

Substituting it into (7.2.1) - (7.2.5) yields

$$\frac{\partial^2\hat{w}}{\partial z^2}+m^2\hat{w}=\frac{\hat{H}}{(c-U)^2}+\left(\frac{1}{c-U}\right)\left(\hat{F}_{1z}-ik\hat{F}_3\right), \tag{7.2.11}$$

where

$$m^2 = \frac{1}{c-U}\frac{d^2U}{dz^2} + \frac{N^2}{(c-U)^2} - k^2 . \qquad (7.2.12)$$

Defining a new variable h as

$$h \equiv \frac{\hat{w}}{c-U} , \qquad (7.2.13)$$

It can be derived from (7.2.11),

$$-2\int_0^\infty c_i(c_r-U)\left[\left|\frac{\partial h}{\partial z}\right|^2 + k^2|h|^2\right]dz = \mathrm{Im}\int_0^\infty \frac{\hat{w}^*\hat{H}}{|c-U|^2}dz + \mathrm{Im}\int_0^\infty h^*\left(\hat{F}_{1z} - ik\hat{F}_3\right)dz .$$

(7.2.16)

Case (i): No forcing

Eq. (7.2.16) is reduced to

$$-2\int_0^\infty c_i(c_r-U)\left[\left|\frac{\partial h}{\partial z}\right|^2 + k^2|h|^2\right]dz = 0 . \qquad (7.2.17)$$

In order for instability to occur, c_i must be greater than 0.

This implies that term $(c_r - U)$ must change sign somewhere between $z = 0$ and ∞ because the term in the square bracket is always positive. Therefore, ***there exists a critical level at which*** $U = c_r$ ***in order for instability to occur in a two-dimensional, nonrotating flow***.

Case (ii): with only thermal forcing, Eq. (7.2.16) reduces to

$$-2\int_0^\infty c_i(c_r-U)\left[\left|\frac{\partial h}{\partial z}\right|^2 + k^2|h|^2\right]dz = \mathrm{Im}\int_0^\infty \frac{\hat{w}^*\hat{H}}{|c-U|^2}dz . \qquad (7.2.18)$$

Assume

$$H = Qe^{i\theta}w. \tag{7.2.19}$$

After substituting Eq. (7.2.19) into Eq. (7.2.18), the right hand side of Eq. (7.2.18) becomes

$$\mathrm{Im}\int_0^\infty \frac{\hat{w}^*\hat{H}}{|c-U|^2}dz = \int_0^\infty \frac{Q|\hat{w}|^2\sin\theta}{|c-U|^2}dz. \tag{7.2.20}$$

If the heating is in phase with vertical velocity everywhere, i.e. $\theta = 0$, then

$$-2\int_0^\infty c_i(c_r-U)\left[\left|\frac{\partial h}{\partial z}\right|^2 + k^2|h|^2\right]dz = \mathrm{Im}\int_0^\infty \frac{\hat{w}^*\hat{H}}{|c-U|^2}\,dz = 0$$

This implies that either $c_i = 0$, where there is no amplification or instability, or $c_r = U$ at certain level, where a *steering* or *critical level* exists.

This leads us to ***Bolton's theorem***: If a diabatic forcing is to generate an amplifying, non-steering level perturbation, the forcing must be somewhat out of phase with the vertical velocity (Bolton, 1980a; Moncrieff 1978).

7.2.2 Miles' Theorem

For a two-dimensional, nonrotating, stratified shear flow with no forcing, Eq. (7.2.14) becomes

$$\frac{\partial}{\partial z}\left[(U-c)^2\frac{\partial h}{\partial z}\right] + \left[N^2 - k^2(U-c)^2\right]h = 0, \tag{7.2.21}$$

with $h(z_1) = h(z_2) = 0$.

If the flow is unstable, then c will be complex and $U - c \neq 0$ for any height z.

Assuming $h = G/\sqrt{U-c}$ and substituting it into the above equation gives

$$c_i \left(\int_{z_1}^{z_2} \left[\left| \frac{\partial G}{\partial z} \right|^2 + k^2 |G|^2 \right] dz + \int_{z_1}^{z_2} \left| \frac{G}{U-c} \right|^2 \left(N^2 - \frac{1}{4} U_z^2 \right) dz \right) = 0 . \qquad (7.2.24)$$

Since the flow is assumed to be unstable, it requires that $c_i > 0$.

The above equation therefore implies that $Ri < 1/4$ at some level between z_1 and z_2, where $Ri \equiv N^2/U_z^2$ is the *Richardson number*.

For instability to occur, it is necessary that $Ri < 1/4$ somewhere in the fluid. On the other hand, *if* $Ri \geq 1/4$ *everywhere in the fluid system, then the fluid system is stable*. This is referred to as *Miles' Theorem*.

7.2.3 Howard's Semicircle Theorem

Consider Eq. (7.2.11) with no forcing,

$$\frac{\partial^2 \hat{w}}{\partial z^2} + m^2 \hat{w} = 0\,, \tag{7.2.25}$$

where

$$m^2 = -\frac{1}{U-c}\frac{d^2U}{dz^2} + \frac{N^2}{(U-c)^2} - k^2\,, \tag{7.2.26}$$

Using the vertical displacement η and substituting its relationship with w,

$$\hat{\eta} = \frac{\hat{w}}{ik(U-c)}\,,. \tag{7.2.27}$$

into Eq. (7.2.25) yields

$$\frac{\partial}{\partial z}\left[(U-c)^2\frac{\partial \hat{\eta}}{\partial z}\right] + \left[N^2 - k^2(U-c)^2\right]\hat{\eta} = 0\,. \tag{7.2.28}$$

The boundary conditions are $\hat{\eta} = 0$ at $z = z_1$ and z_2.

Multiplying Eq. (7.2.28) by the conjugate of $\hat{\eta}$ (i.e. $\hat{\eta}^*$) and then integrating from z_1 to z_2 leads to

$$\int_{z_1}^{z_2} (U-c)^2\left(\left|\frac{\partial \hat{\eta}}{\partial z}\right|^2 + k^2|\hat{\eta}|^2\right)\mathrm{dz} - \int_{z_1}^{z_2} N^2|\hat{\eta}|^2\,dz = 0\,. \tag{7.2.29}$$

Substituting $c = c_r + ic_i$ into the above equation and then separating the real and imaginary parts yields

$$\text{Real Part} = \int_{z_1}^{z_2}\left[(U-c_r)^2 - c_i^2\right] R\,\mathrm{dz} - \int_{z_1}^{z_2} N^2\,|\hat{\eta}|^2\,dz = 0 \tag{7.2.30}$$

$$\text{Imaginary Part} = 2c_i \int_{z_1}^{z_2} (U - c_r)\, R \; \mathrm{dz} \; = 0 \tag{7.2.31}$$

where

$$R = \left| \frac{\partial \hat{\eta}}{\partial z} \right|^2 + k^2 |\hat{\eta}|^2 . \tag{7.2.32}$$

Again, for instability to occur, we require $c_i > 0$. In turn, with (7.2.32), Eq. (7.2.31) requires that

$$\int URdz = c_r \int Rdz . \tag{7.2.33}$$

Equations (7.2.30) and (7.2.33) imply that

$$\int U^2 Rdz = \left(c_r^2 + c_i^2\right) \int Rdz + \int N^2 |\hat{\eta}|^2 dz . \tag{7.2.34}$$

Now supposing $a \le U(z) \le b$, we then have

$$\left\{ [c_r - (a+b)/2]^2 + c_i^2 - [(a-b)/2]^2 \right\} \int Rdz + \int N^2 |\hat{\eta}|^2 dz \le 0 . \tag{7.2.35}$$

Since the last term on the left side of the above equation and the integration of R with respect to z are both positive, we require that

$$[c_r - (a+b)/2]^2 + c_i^2 \le [(a-b)/2]^2 . \tag{7.2.36}$$

This leads us to the *Howard semicircle theorem*: *The complex phase speed, c, of an unstable normal mode must lie within the semicircle enclosed by U_{min} (i.e. a) and U_{max}* (i.e. *b*). The Howard semicircle theorem can also be sketched as shown in Fig. 7.3.

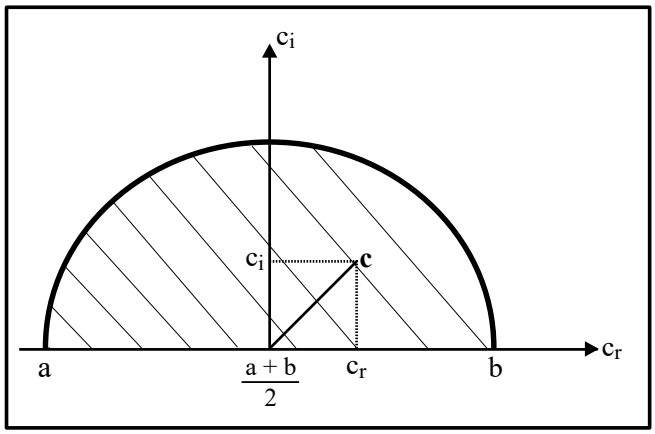

Fig. 7.3: A sketch of the Howard's semicircle theorem.

7.3 Static, Conditional, and Convective Instabilities

7.3.1 Static Instability

- *Static instability* is also referred to in the literature as *buoyant instability* and *gravitational instability*, and describes an atmospheric state in which an air parcel will accelerate away from its original level due to the density difference between itself and its environment.

- It can be derived that

$$N^2 = \frac{g}{\bar{\theta}}\frac{\partial \bar{\theta}}{\partial z} = \frac{g}{T}(\Gamma_d - \gamma), \tag{7.3.2}$$

where

N : *Brunt-Vaisala* or *buoyancy frequency*,

$\gamma \equiv -\partial T / \partial z$: observed *environmental or actual lapse rate*

$\Gamma_d = g / c_p$: *dry lapse rate*.

The overbar represents values of the environmental air.

The stability criteria for the displacement of a dry or unsaturated air parcel are

$\gamma < \Gamma_d$: *absolutely stable*,
$\gamma = \Gamma_d$: *dry neutral*, (7.3.3)
$\gamma > \Gamma_d$: *dry absolutely unstable*.

The vertical motion of the air parcel follows

$$\frac{Dw}{Dt} = \frac{D^2\delta z}{Dt^2} = -\frac{1}{\rho}\frac{\partial p}{\partial z} - g\,, \tag{7.3.4}$$

where ρ and p are the density and pressure of the air parcel, respectively.

According to parcel theory, the pressure of the air parcel adjusts immediately to the pressure of its environment ($\bar{p}$), i.e. $p = \bar{p}$, which leads to

$$\frac{Dw}{Dt} = \frac{D^2\delta z}{Dt^2} = g\left(\frac{\bar{\rho} - \rho}{\rho}\right) \equiv B\,, \tag{7.3.5}$$

where *B* is the *buoyancy* or the buoyancy force per unit mass, and the overbar denotes the environmental value. In deriving the above equation, we have assumed the environmental atmosphere is in hydrostatic balance.

Thus, (7.3.5) indicates that the vertical acceleration of the air parcel is controlled by the ***buoyancy force***, $g[(\bar{\rho} - \rho)/\rho]$. It can be derived that the buoyancy force (the right hand side of (7.3.5)), is approximately equal

to $g[(\theta-\bar{\theta})/\bar{\theta}]$. At $z=0$, the air parcel is assumed to have the same potential temperature (θ) as that of its environment ($\bar{\theta}$).

It can be derived

$$\frac{D^2\delta z}{Dt^2}+\mathrm{N}^2\delta z=0. \qquad (7.3.6)$$

The Brunt-Vaisala frequency measures the static stability of the air parcel's environment and is related to the change of the air parcel's buoyancy in relation to height,

$$N^2=-\frac{\partial B}{\partial z}=\frac{g}{\bar{\theta}}\frac{\partial\bar{\theta}}{\partial z}. \qquad (7.3.7)$$

It can be easily proven that the criteria for static stability, static neutrality, and static instability are: $N^2>0$, $N^2=0$, and $N^2<0$, respectively.

The static instability acts on a horizontal scale of tens to thousands of meters. Static and shear instability produce most of the small-scale turbulence in the troposphere.

The stability criteria for dry air may also be determined by the vertical gradient of the environmental potential temperature:

$$\frac{\partial \bar{\theta}}{\partial z} \begin{cases} > 0 & \text{absolute stable} \\ = 0 & \text{dry neutral} \\ < 0 & \text{dry absolute unstable,} \end{cases} \tag{7.3.8}$$

In the above criteria, $\partial\bar{\theta}/\partial z$ can be replaced by the dry Brunt-Vaisala frequency (N). The dry absolute instability is also referred to as *dry gravitational instability* in the literature.

- The vertical acceleration is contributed by the dynamic pressure (p_d') and buoyancy pressure (p_b'). The dynamical pressure arises from the flow field differences created by the disturbance, and buoyancy pressure is generated by the vertical buoyancy gradient.
- Taking these effects into consideration, the vertical momentum equation can be written as

$$\frac{Dw}{Dt} = -\frac{1}{\rho_o}\frac{\partial p_d'}{\partial z} + \left(B - \frac{1}{\rho_o}\frac{\partial p_b'}{\partial z} \right), \tag{7.3.10}$$

$$-\frac{1}{\rho_o}\nabla^2 p_d' = |D|^2 - |\zeta|^2, \tag{7.3.11a}$$

$$-\frac{1}{\rho_o}\nabla^2 p_b' = -\frac{\partial B}{\partial z}. \tag{7.3.11b}$$

where

$|D|$: total deformation and

ζ : 3D vorticity vector.

- The first term on the right side of (7.3.10) is due to the dynamic perturbation pressure, which is independent of the thermodynamic base state.
- The buoyancy should include both terms inside the bracket on the right side of (7.3.10) (Doswell and Markowski 2004).

* It has been proposed and observed in the real atmosphere that ***moist absolute instability*** may be created and maintained as mesoscale convective systems develop (Bryan and Fritsch 2000).

- A strong, mesoscale, nonbuoyancy-driven ascent, such as mechanical lifting along surface-based outflow layers, frontal zones, or an elevated terrain, may bring a conditionally unstable environmental layer to saturation faster than small-scale, buoyancy-driven convective elements are able to overcome the unstable state.
- In addition, the lifting of a *moist absolutely unstable layer* (*MAUL*) tends to warm the environment, causing a reduction in the temperature difference between the environment and vertically displaced parcels, and thereby decreasing the buoyancy of convective parcels and helping to maintain the MAUL (Bryan and Fritsch 2000).

- Figure 7.4 illustrates how, in an idealized convective system, a MAUL forms ahead of a density current created through slab convective overturning.

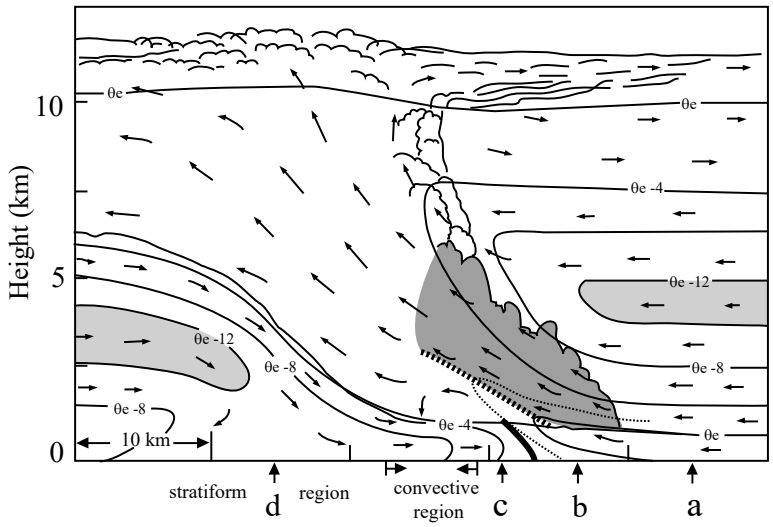

Fig. 7.4: A schematic of the formation of a MAUL through slab convective overturning. Wind vectors relative to the outflow boundary are denoted by arrows, cloud boundaries are denoted by scalloped lines, θ_e contours (every 4 K) are denoted by solid lines, the outflow boundary or frontal zone is denoted by heavy solid line, midlevel layer of low θ_e is highlighted by light shading, and the MAUL is depicted by dark shading. (From Bryan and Fritsch 2000)

7.3.2 Conditional Instability

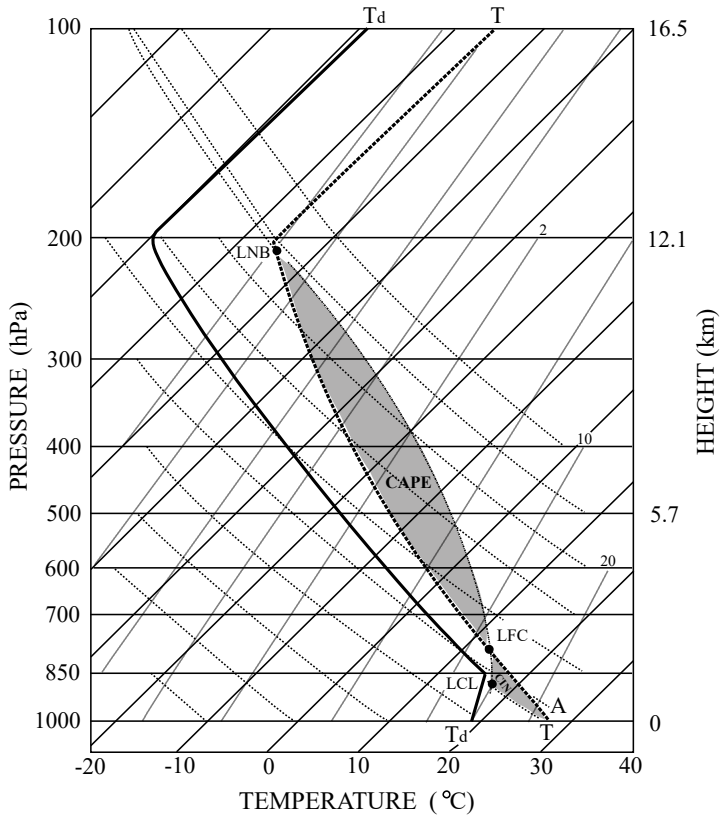

Fig. 7.5: Example of a sounding with conditional instability displayed on a *skew-T log-p* thermodynamic diagram. The lifting condensation level (LCL), level of free convection (LFC), and level of neutral buoyancy (LNB) for the air parcel originated at A are denoted in the figure. The convective available potential energy (CAPE) is the area enclosed by the temperature curve (thick dashed line) and moist adiabat (dot-dashed curve) in between LFC and LNB, while the convective inhibition is the area enclosed the temperature curve and dry adiabat (below LCL) and moist adiabat (above LCL) in between the surface and the LFC.

Lifting condensation level (*LCL*)

Level of free convection (*LFC*).

Level of neutral buoyancy (LNB)

Convective available potential energy (*CAPE*):

$$CAPE = \int_{z_{LFC}}^{z_{LNB}} B\, dz = \int_{z_{LFC}}^{z_{LNB}} g\left(\frac{\overline{\rho} - \rho}{\rho}\right) dz = \int_{z_{LFC}}^{z_{LNB}} g\left(\frac{T - \overline{T}}{\overline{T}}\right) dz = \int_{z_{LFC}}^{z_{LNB}} g\left(\frac{\theta - \overline{\theta}}{\overline{\theta}}\right) dz$$

.

(7.3.17)

The *moist adiabatic lapse rate*

$$\Gamma_s \equiv -\frac{dT}{dz} = \frac{\Gamma_d}{1 + (L/c_p)(dq_{vs}/dT)}, \qquad (7.3.18)$$

where Γ_d is the dry adiabatic lapse rate,

L is the latent heat of condensation or sublimation, and

q_{vs} is the saturation water vapor mixing ratio.

CIN: The negative area represents the energy needed to lift an air parcel to its *LFC* and is also known as the *convective inhibition CIN*. Mathematically, *CIN* may be defined as

$$CIN = -\int_{z_i}^{z_{LFC}} g\left(\frac{T - \overline{T}}{\overline{T}}\right) dz\,. \qquad (7.3.22)$$

Thus, the *CIN* is the energy required to lift an air parcel vertically and pseudoadiabatically to its level of free convection.

$w_{\max} = \sqrt{2CAPE}$.

When rain evaporates in sub-saturated air or solid precipitate (snow or hail) melts at the melting level, a downdraft will be generated by the cooled air. The maximum downdraft may be estimated as $-w_{\max} = \sqrt{2DCAPE_i}$, where $DCAPE_i$ is the *downdraft convective available potential energy* and is defined as

$$DCAPE_i = -\int_{z_i}^{z_s} g\left(\frac{T-\overline{T}}{\overline{T}}\right) dz, \qquad (7.3.23)$$

where z_s is normally the surface or the level at which an air parcel descends from the original level z_i, allowing a neutral buoyancy to be achieved. Cooling the parcel to saturation via the wet-bulb process and then descending it saturated- or pseudo-adiabatically, leaving enough evaporation to keep the air parcel saturated will allow one to obtain the parcel temperature (e.g. Emanuel 1994).

- The criterion for conditional instability may also be determined via the vertical gradient of the *saturation equivalent potential temperature* (θ_e^*), which is defined as the equivalent potential temperature of a hypothetically saturated atmosphere. This hypothetical atmosphere has the same thermal structure as the actual atmosphere.

- In other words, the θ_e^* can be defined as the equivalent potential temperature the air parcel would have if it were saturated at the same pressure and temperature,

$$\theta_e^* = \theta \exp(Lq_{vs} / c_p T)\,. \qquad (7.3.24)$$

The criterion for conditional instability can also be determined via the vertical gradient of the *saturation equivalent potential temperature* (θ_e^*) which is defined as the equivalent potential temperature of a hypothetically saturated atmosphere at the initial level. This hypothetical atmosphere has been set to mimic the thermal structure of the actual atmosphere. In other words, θ_e^* can be defined as the equivalent potential temperature that the air parcel would have if it were saturated initially at the same pressure and temperature, and can be calculated by

$$\theta_e^* = \theta\, e^{Lq_{vs}/c_pT}\,. \qquad (7.3.17)$$

In order to derive the criterion for conditional instability, we consider an air parcel lifted from $z_o - \delta z$ to z_o . At $z_o - \delta z$, the air parcel is assumed to have the same potential temperature as that of the environment, $\overline{\theta} - (\partial\overline{\theta}/\partial z)\eta$, where $\overline{\theta}$ is the potential temperature of the environmental air at z_o , and $\eta = \delta z$ is the vertical displacement. The potential temperature of the air parcel experiences a change of $\delta\theta$ when it is lifted from $z_o - \eta$ to z_o , i.e. $[\overline{\theta} - (\partial\overline{\theta}/\partial z)\eta] + \delta\theta$. Thus, the buoyancy of the air parcel at z_o is

$$b = g\left(\frac{\theta - \overline{\theta}}{\overline{\theta}}\right) = -\frac{g}{\overline{\theta}}\frac{\partial\overline{\theta}}{\partial z}\eta + g\frac{\delta\theta}{\overline{\theta}}\,. \qquad (7.3.18)$$

Substituting the heating rate ($\dot{q}$) from latent heat release, $\dot{q} = -L(Dq_{vs}/Dt)$, into (2.2.5) gives

$$\frac{\delta\theta}{\overline{\theta}} \approx -\delta\left(\frac{Lq_{vs}}{c_pT}\right) \approx -\frac{\partial}{\partial z}\left(\frac{Lq_{vs}}{c_pT}\right)\eta\,. \qquad (7.3.19)$$

Substituting (7.3.19) into (7.3.18) and using the definition of θ_e^* leads to

$$b \approx -\left(\frac{g}{\overline{\theta}_e^*}\frac{\partial\overline{\theta}_e^*}{\partial z}\right)\eta\,. \qquad (7.3.20)$$

Substituting the above equation into (7.3.2) for a moist atmosphere, gives us

$$\frac{D^2\eta}{Dt^2} + \left(\frac{g}{\overline{\theta}_e^*}\frac{\partial\overline{\theta}_e^*}{\partial z}\right)\eta = 0\,. \qquad (7.3.21)$$

Therefore, *the conditional stability criterion for a saturated layer of air becomes*

$$\frac{\partial\overline{\theta}_e^*}{\partial z} \begin{cases} > 0 & \text{conditionally stable} \\ = 0 & \text{conditionally neutral} \\ < 0 & \text{conditionally unstable} \end{cases} \qquad (7.3.22)$$

Note that in addition to $\partial\overline{\theta}_e^*/\partial z < 0$, the release of conditional instability requires the air parcel to be lifted above its LFC. This requirement is not included in the above derivation (e.g.

Sherwood 2000; Schultz et al. 2000). Parcel theory also neglects the effects of mass continuity and pressure perturbation (Xu 1986), as also known from dry static instability.

- As shown above, it can be derived

$$\frac{D^2\eta}{Dt^2}+\left(\frac{g}{\overline{\theta}_e^*}\frac{\partial\overline{\theta}_e^*}{\partial z}\right)\eta=0$$

Therefore, the conditional stability criterion for a saturated layer of air becomes

$$\frac{\partial\overline{\theta}_e^*}{\partial z}\begin{cases}>0 & \text{conditionally stable}\\ =0 & \text{conditionally neutral}\\ <0 & \text{conditionally unstable}\end{cases} \qquad (7.3.29)$$

Based on the above discussion, there exist six static stability states for dry and moist air:

1) absolutely stable $\gamma<\Gamma_s$,
2) saturated neutral $\gamma=\Gamma_s$,
3) conditionally unstable $\Gamma_s<\gamma<\Gamma_d$, (7.3.30)
4) dry neutral $\gamma=\Gamma_d$,
5) dry absolute unstable $\gamma>\Gamma_d$,
6) moist absolutely unstable $\gamma_s>\Gamma_s$.

➢ Note that parcel theory has been used to assess the instabilities discussed above. We must note that this theory is generally developed in terms of buoyancy, namely the density or temperature difference between an ascending air parcel and its environmental air. This makes parcel theory incapable of dealing with instabilities that depend on horizontal pressure gradients, such as baroclinic and barotropic instabilities (Emanuel 1994).

- In addition, parcel theory does not take into account the following:
  (1) the entrainment of the environmental air
  (2) the compensating vertical motions of the environmental air in response to the intrusion of clouds, and
  (3) the effect of condensate on buoyancy.

The first effect tends to reduce the buoyancy. It may be assumed that as saturated cloud air ascends a distance δz, a mass δm of environmental air is entrained. This will require heat from the air parcel (cloudy air) to warm this entrained air. In addition, the condensed water in the cloud will evaporate in response to the *entrainment* of drier environmental air. Taking these effects into account, (7.3.19) becomes

$$\frac{\delta\theta}{\bar{\theta}} \approx -\frac{\partial}{\partial z}\left(\frac{Lq_{vs}}{c_pT}\right)\delta z - \left(b + \frac{L}{c_pT}(q_{vs} - \bar{q})\right)\frac{\delta m}{m}, \qquad (7.3.31)$$

where $\delta z = \eta$ and $\bar{q}$ is the mixing ratio of the entrained environmental air.

The effect of compensating vertical motions of the environmental air can be improved by the *slice method* (Bjerknes 1938), which takes into account of the area of compensated downward motion through mass continuity in estimating the stability.

Finally, the melting of snow or evaporative cooling of rainfall may also reduce the buoyancy. Representing these effects more completely and accurately would normally require the use of a numerical model to solve the mathematical problem involving (7.3.31).

7.3.3 Potential Instability

- *Potential instability* is also referred to as *convective instability* in the literature, and describes a condition in which an atmospheric layer becomes unstable statically after lifting.
- It is based on layer theory. An entire atmospheric layer may be lifted by a density current, a broad mountain range, a frontal surface, or a cyclone. Under these situations, *layer theory* is more appropriate for assessing the instability of the lifted layer, as opposed to *parcel theory* for conditional instability.

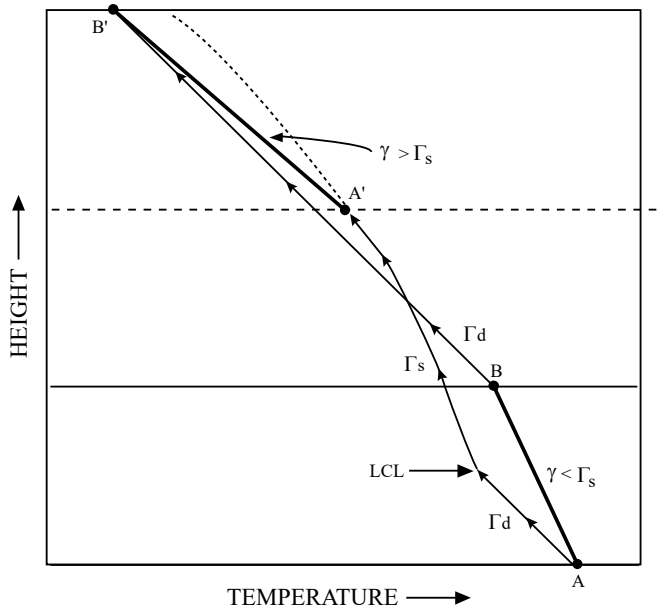

Fig. 7.6: Illustration of potential (convective) instability by lifting an initially absolute stable layer AB with $\partial\overline{\theta}_e/\partial z < 0$. The top of the layer (B) follows a dry adiabat to saturation at B', while the bottom of the layer becomes saturated earlier and then follows moist adiabat to A'. The lapse rate of the final saturated layer (A'B') is greater than the moist adiabat, thus is unstable. (Adapted after Darkow 1986)

- [Layer Theory] In order to understand potential instability, we first consider a dry layer of the atmosphere extending from pressure level p_1 up to p_2, and assume that:

(a) the mass is conserved within the layer and
(b) the atmosphere is in hydrostatic balance.

Since the pressure difference is directly proportional to the mass per unit area contained in the air column, it can be approximated by $p_1 - p_2 = \rho_{av} g \delta z$, where ρ_{av} is the averaged air density of the layer and $\delta z = z_2 - z_1$.

Therefore, layer lifting (sinking) tends to make the column stretch (shrink), because ρ_{av} decreases (increases) with height. It follows that $\partial \bar{\theta} / \partial z$ decreases (increases) for the lifting (sinking) of a dry or unsaturated layer with no condensation since $\delta \bar{\theta} \approx (\partial \bar{\theta} / \partial z) \delta z$ and $\delta \bar{\theta}$ is conserved.

In other words, lifting tends to make a layer less stable in a dry or unsaturated atmosphere, while sinking tends to make the layer more stable.

One exception to this occurs when the layer of air is neutrally stable, in which case $\partial \bar{\theta} / \partial z = 0$ before and after the vertical displacement.

- The situation is completely different if saturation occurs during the layer lifting, since lifting may make an initially stable layer absolutely unstable.

The process leading to instability ($\gamma > \Gamma_s$) can be illustrated by using a thermodynamic diagram, such as Fig. 7.6.

We lift an initially absolutely stable layer ($\gamma < \Gamma_s$) with $\partial \bar{\theta}_e / \partial z < 0$. In this situation, the top of the layer follows a dry adiabat. After lifting, the layer ($A'B'$) becomes saturated and unstable because $\gamma > \Gamma_s$. Similar graphical operations indicate that an initially

absolutely stable layer can become saturated and stable (neutral) when $\partial\overline{\theta}_e / \partial z > 0$ ($\partial\overline{\theta}_e / \partial z = 0$).

Thus, the criteria for potential (convective) instability can be expressed in terms of the equivalent potential temperature, since this is a conserved quanity for the moist layer.

- The criteria for potential (convective) instability may be expressed in terms of the equivalent potential temperature.

$$\frac{\partial\overline{\theta}_e}{\partial z} \begin{cases} > 0 & \text{potentially stable} \\ = 0 & \text{potentially neutral} \\ < 0 & \text{potentially unstable} \end{cases} \qquad (7.3.31)$$

7.4 Kelvin-Helmholtz Instability

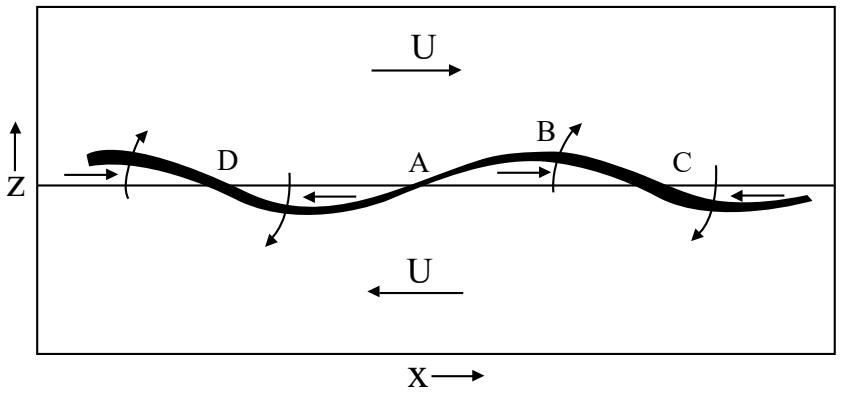

Fig. 7.8: A sketch illustrates the growth of a sinusoidal disturbance to an initially uniform vortex sheet (dashed) with positive vorticity normal to the paper. The local strength of the vortex sheet is represented by the thickness of the sheet. The curved arrows indicate the direction of the self-induced movement of the vorticity in the sheet, and show (a) the accumulation of vorticity at points like *A* and (b) the general rotation about points like *A*, which together lead to exponential growth of the disturbance. (Adapted after Batchelor 1967 and Drazin and Reid 1981)

Fig. 7.9: An example of breaking Kelvin-Helmholtz waves in clouds (billow clouds) formed over Laramie, Wyoming, USA. (Photo by Brooks Martner, NOAA Environmental Technology Laboratory)

Criterion of the K-H instability is based on Miles' theorem: $Ri < 1/4$ somewhere in the fluid is a necessary condition for instability to occur.

7.5 Inertial Instability

- For typical atmospheric conditions $N^2 > 0$, the vertically displaced air parcel either returns to its original position or acts to stabilize vertical displacement.
- Analogous to the static instability, rotation tends to return the horizontally displaced air parcel to its original position or stabilize the displacement.
- This is similar to how buoyancy tends to return or stabilize the vertically displaced air parcel. This type of instability is called *inertial instability*.
- We have *inertial instability* if the horizontally displaced parcel accelerates away from its original position.

The equations of motion for an inviscid, Boussinesq fluid in the cylindrical polar coordinates (r, θ, z) may be written as

$$\frac{Du}{Dt} - \frac{V^2}{r} = -\frac{1}{\rho_o}\frac{\partial p}{\partial r}, \tag{7.5.1}$$

$$\frac{DV}{Dt} + \frac{uV}{r} = -\frac{1}{\rho_o r}\frac{\partial p}{\partial \theta} = 0, \tag{7.5.2}$$

$$\frac{Dw}{Dt} = -\frac{1}{\rho}\frac{\partial p}{\partial z}, \tag{7.5.3}$$

where r is the radius or distance from the axis of rotation, (u, V, w) are the radial, azimuthal (tangential) and vertical velocities, respectively, and the total derivative is defined as $D/Dt \equiv \partial/\partial t + u\,\partial/\partial r + w\,\partial/\partial z$.

The equation of mass conservation is

$$\frac{\partial u}{\partial r} + \frac{u}{r} + \frac{\partial w}{\partial z} = 0. \qquad (7.5.4)$$

Since the tangential velocity is related to *angular momentum* per unit mass (M) and angular velocity (Ω) by $M \equiv Vr = \Omega r^2$, Eq. (7.5.2) can be rewritten as

$$\frac{DM}{Dt} = \frac{D(Vr)}{Dt} = 0, \qquad (7.5.5)$$

Thus the angular momentum is conserved for an axisymmetric motion in an inviscid fluid. Note that the circumference around the circle of radius r is $2\pi M$.

The mean state is assumed to have no radial acceleration. In other words, it is said to be in *cyclostrophic flow* balance (e.g. see Holton 2004), meaning that the pressure gradient force in the environment is balanced by the centrifugal force

$$-\frac{\overline{M}^2}{r^3} = -\frac{\overline{V}^2}{r} = -\frac{1}{\rho_o}\frac{\partial \overline{p}}{\partial r}. \qquad (7.5.6)$$

According to parcel theory, the motion does not perturb the pressure field of the environment. It is from this theory that we make our assumptions.

Thus, (7.5.1) becomes

$$\frac{Du}{Dt} = -\frac{1}{\rho_o}\frac{\partial p}{\partial r} + \frac{\overline{V}^2}{r} = \frac{1}{r^3}\left(M^2 - \overline{M}^2\right). \qquad (7.5.7)$$

To illustrate the concept of inertial stability, let us consider that the square of environmental angular momentum ($\overline{M}^2$) increases with the radius and the vortex circular motion is assumed to be in *solid body rotation*, as shown in Fig. 7.10.

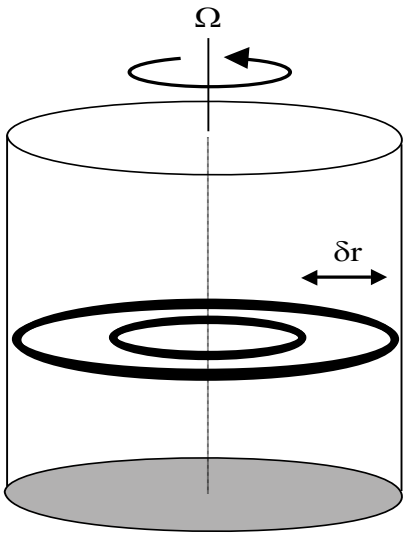

Fig. 7.10: Schematic representation of an inertially stable system of fluid confined by a rotating cylinder. The square of environmental angular momentum ($\overline{M} \equiv u_\theta r = \Omega r$) is assumed to increase with radius. (Adapted after Emanuel 1994)

- Now consider a ring of fluid displaced radially outward.
- The conservation of angular momentum ($M \equiv Vr = \Omega r^2$) provides less angular velocity (Ω) and centrifugal force for the tube than that which is required to balance the local pressure gradient force in the new position. This forces the air tube to accelerate back toward its original position, creating an inertially stable system.
- It can be derived,

$$\frac{Du}{Dt} = -\frac{1}{r_o^3}\frac{\partial \overline{M}^2}{\partial r}\delta r \qquad (7.5.8)$$

at $r_o + \delta r$.

- Therefore, the fluid motion is *stable* if $\overline{M}^2$ increases with the radius from the axis of rotation.
- This leads to the Rayleigh (1916) criteria for inertial stability, neutrality, and instability for a homogeneous, incompressible and inviscid circular vortex motion

$$\frac{\partial \overline{M}^2}{\partial r} \begin{cases} > 0 & \text{inertially stable} \\ = 0 & \text{inertially neutal} \\ < 0 & \text{inertially unstable} \end{cases} \qquad (7.5.9)$$

- It can be shown that a *Rankine vortex*, where $V = ar$ for $r \le r_c$ and $V = b/r$ for $r > r_c$, and a and b are constants, is inertially stable for $r \le r_c$ and neutral for $r > r_c$.
- Note that a Rankine vortex is often used to represent the circulation of a tornado vortex core or a tropical cyclone in numerical modeling simulations, as in the so-called *bogusing* technique.

* Based on this information, the criteria for inertial stability, neutrality, and instability are:

$$f\frac{\partial \overline{M}}{\partial x} = f\left(\frac{\partial v_g}{\partial x} + f\right) \begin{matrix} > 0 & \text{inertially stable} \\ = 0 & \text{inertially neutral} \\ < 0 & \text{inertially unstable} \end{matrix} \qquad (7.5.15)$$

In the Northern Hemisphere ($f > 0$), the flow is inertially stable if the absolute vorticity of the basic flow, $\partial \overline{M} / \partial x = \partial v_g / \partial x + f$, is positive.

7.6 Symmetric Instability

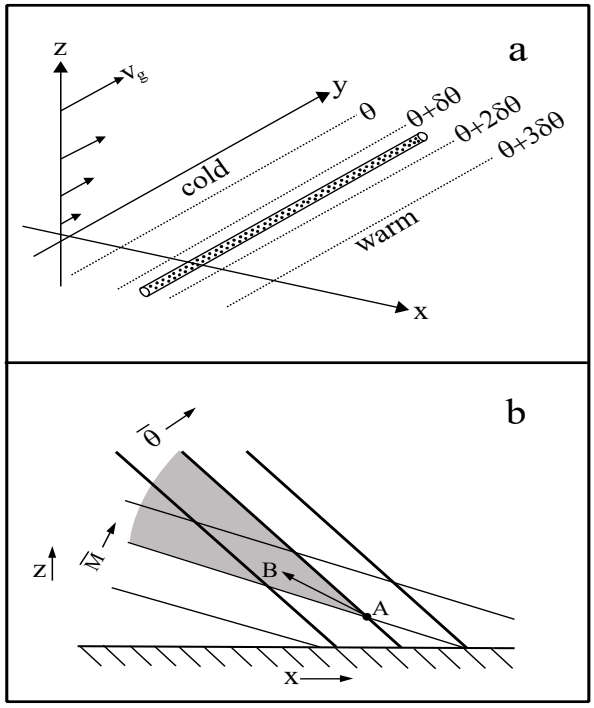

Fig. 7.11: A schematic of a mean state with symmetric instability. (a) A meridional, steady baroclinic flow. The unidirectional geostrophic wind v_g is in thermal wind balance. One may imagine an idealized broad front is aligned with y-axis and located in between the cold and warm region. Under this situation, v_g is the along-front wind. (b) The $\overline{M}$ and $\overline{\theta}$ surfaces on the *x-z* plane are tilted such that both of them increase upward and eastward. Displacement of an air parcel upward anywhere within the shaded area from point A is symmetrically unstable (Adapted after Houze 1993).

- As discussed in previous sections, if a dry or unsaturated atmosphere satisfies the criteria for static (gravitational) stability ($N^2 > 0$) and inertial stability ($f\,\partial\overline{M}/\partial x = f\,(\partial v_g/\partial x + f) > 0$) separately, then an air parcel displaced either vertically or horizontally in the atmosphere will return to its original position.

- However, under certain conditions, it is possible for an air parcel to accelerate away from its original position if it is displaced along a slantwise path.
- This type of instability is called *symmetric instability*, and is called so because the basic state and perturbations are independent of the horizontal coordinates. Due to this reason, both $\partial/\partial x = 0$ and $\partial/\partial y = 0$ have been used to refer to this state in the literature. In the previous section, we assumed $\partial/\partial y = 0$ and thus defined $M = v + fx$.
- On the other hand, if we assume $\partial/\partial x = 0$, then the absolute momentum may be defined as $M = u - fy$ and the inertial instability criterion becomes $-f\,\partial\overline{M}/\partial y = f\,(f - \partial u_g/\partial y) < 0$. Symmetric instability has also been referred to as *isentropic inertial instability* in the literature.
- In a dynamic sense, static, potential, inertial, and symmetric instabilities are very closely related. Each of the instabilities can be thought of as resulting from an unstable distribution of body forces acting on a fluid element. The responsible body forces are the gravitational force for static and potential instabilities, centrifugal force for inertial instability, and a combination of gravitational forces in the vertical and centrifugal forces in the horizontal for symmetric instability. Due to the combination of these two forces, symmetric instability occurs when the motion is slantwise.

7.6.1 Dry Symmetric Instability

- The symmetric instability in a dry atmosphere can be understood by applying the parcel argument. For convenience, consider a Boussinesq fluid in which the basic flow and disturbances are independent of the *y* direction, i.e. $\partial/\partial y = 0$, as was assumed earlier in the derivation of criterion for inertial instability. The air parcel can now be viewed as a tube of air extending infinitely along the *y*-axis.
- To demonstrate that symmetric instability may occur when the basic flow is both statically and inertially stable, we consider the mean state of the atmosphere as illustrated in Fig. 7.11.
- The basic flow is also assumed to be in hydrostatic and geostrophic balance, i.e. in thermal wind balance,

$$f\frac{\partial v_g}{\partial z} = \frac{g}{\theta_o}\frac{\partial \overline{\theta}}{\partial x} \quad , \qquad (7.6.1)$$

  where $\overline{\theta}(x)$ and θ_o are the mean potential temperature and a constant reference potential temperature, respectively.
- Imagine that an idealized front is aligned with the y-axis and located between the cold and warm regions as sketched in Fig. 7.11a. Under this situation, v_g becomes the along-front wind. The $\overline{M}$ and $\overline{\theta}$ surfaces on the *x*-*z* plane are tilted such that both $\overline{\theta}$ and $\overline{M}$ increase upward and eastward (Fig. 7.11b). Since $\partial\overline{\theta}/\partial z > 0$, an air parcel

displaced upward (downward) from A will have a lower (higher) value of $\bar{\theta}$ than its environment, assuming no perturbation of the environment by the parcel and immediate adjustment of the parcel's pressure to that of its environment. Thus, the parcel density is greater (smaller) than the environment for upward (downward) motion and results in negative buoyancy, which forces the parcel to accelerate back to its origin. Analogously, since $\partial \overline{M} / \partial x > 0$, an air parcel displaced horizontally in the negative direction from point *A* in Fig. 7.11 acquires a positive value of ($M - \overline{M}$) and is accelerated back toward A, according to Eq. (7.5.10).

- Displacement of an air parcel along a $\overline{M}$ surface, as shown in Fig. 7.11, will not cause the parcel to experience any horizontal acceleration since its M value is conserved in the displacement. Similarly, a parcel displaced along the $\bar{\theta}$ surface will not experience any vertical acceleration. However, displacement of an air parcel upward anywhere within the shaded wedge, will subject the parcel to an upward and leftward acceleration in the direction of its initial displacement since $\bar{\theta}$ decreases and $\overline{M}$ increases along the displacement AB. This is called *symmetric instability* or more specifically *dry symmetric instability*.
- Dry symmetric instability can also be viewed as either dry static (gravitational) instability on a $\overline{M}$ surface, i.e. $\partial \bar{\theta} / \partial z \big|_{M_g} < 0$, or inertial instability on an isentropic surface, i.e. $\partial \overline{M} / \partial x \big|_{\bar{\theta}} < 0$. Thus, any

slantwise displacement within the wedge expanded between $\overline{M}$ and $\overline{\theta}$ may release the symmetric instability.

- The occurrence of symmetric instability requires

$$-\left.\frac{\partial z}{\partial x}\right|_{\overline{\theta}} > -\left.\frac{\partial z}{\partial x}\right|_{\overline{M}}. \tag{7.6.2}$$

Based on coordinate transformation (e.g. Holton 2004), we have

$$\left.\frac{\partial z}{\partial x}\right|_{\overline{\theta}} = -\frac{\partial \overline{\theta}/\partial x}{\partial \overline{\theta}/\partial z}; \qquad \left.\frac{\partial z}{\partial x}\right|_{\overline{M}} = -\frac{\partial \overline{M}/\partial x}{\partial \overline{M}/\partial z}. \tag{7.6.3}$$

Substituting (7.6.3) into (7.6.2) leads to

$$\frac{(\partial \overline{\theta}/\partial x)(\partial \overline{M}/\partial z)}{(\partial \overline{\theta}/\partial z)(\partial \overline{M}/\partial x)} > 1. \tag{7.6.4}$$

* The necessary condition for the dry symmetric instability

$$\frac{R_i}{f}\left(\frac{\partial v_g}{\partial x} + f\right) < 1, \text{ or} \tag{7.6.5a}$$

$$R_i < \frac{f}{\zeta_{ga}}, \tag{7.6.5b}$$

where $R_i = N^2/(\partial v_g/\partial z)^2$ is the Richardson number and ζ_{ga} is the geostrophic absolute vorticity.

* We find that symmetric instability is favored by low static stability, strong basic state wind shear, and anticyclonic relative vorticity. If there no horizontal wind shear exists, the above criterion is reduced to $R_i < 1$.

An alternative method to derive the criterion for dry symmetric instability is to evaluate a small displacement δx along a constant θ surface, i.e. $(\delta x)_\theta$, and then to use Eqs. (7.5.10) and (7.5.11) with the assumption of thermal wind balance (7.6.1), which leads to

$$\frac{D^2(\delta x)_\theta}{Dt^2} + f^2\left[\frac{\zeta_{ga}}{f} - \frac{1}{R_i}\right](\delta x)_\theta = 0\,. \qquad (7.6.6)$$

The derivation of the above equation is similar to that of Eq. (7.5.14) for inertial instability. The necessary condition for symmetric instability to occur requires the term in square bracket of (7.6.6) to become negative, which leads to the identical criterion in Eq. (7.6.5).

In order to gain a better understanding of the circulation that occurs at the onset of symmetric instability, we can perform a linear stability analysis of the highest unstable mode (e.g. Emanuel 1979; Emanuel and Raymond 1984). For simplicity, we may assume a viscous fluid flow on an *f* plane is confined between two infinite planes which are separated by a vertical distance *H*. The basic state wind, $\overline{V}$, is in the *y* direction and is given by

$$\overline{V}(x,z) = \overline{V}_x\, x + \overline{V}_z\, z\ , \qquad (7.6.7)$$

where $\overline{V}_x$ and $\overline{V}_z$ are the constant vertical and horizontal wind shears, respectively. We also assume the basic flow is in thermal wind balance, which determines the potential temperature

$$\bar{\theta}(x,z) = \frac{\theta_o}{g}\left(N^2 z + \mathrm{f}\bar{V}_z x\right), \tag{7.6.8}$$

where θ_o is a constant reference potential temperature and N is the Boussinesq form of the basic-state buoyancy (Brunt-Vaisala) frequency defined as $(g/\theta_o)\partial\theta/\partial z$. We may also assume that the isentropic surfaces are horizontal, which allows us to apply the hydrostatic assumption to the perturbed flow. This is a reasonable assumption since the slope of isentropic surfaces represented by $f\bar{V}_z/N^2$ has a typical value of about 0.01. The horizontal diffusion for the perturbed flow is negligible, based on viscous Boussinesq approximation and hydrostatic assumption. The perturbations about the basic state are also assumed to be independent of *y*, as are the perturbations about the basic flow.

The linearized perturbation equations for the above flow may be written as

$$\frac{\partial u'}{\partial t} = -\frac{1}{\rho_o}\frac{\partial p'}{\partial x} + fv' + \nu\frac{\partial^2 u'}{\partial z^2}, \tag{7.6.9}$$

$$\frac{\partial v'}{\partial t} + w'\bar{V}_z = -\zeta_{ga}u' + \nu\frac{\partial^2 v'}{\partial z^2}, \tag{7.6.10}$$

$$\frac{1}{\rho_o}\frac{\partial p'}{\partial z} = b', \tag{7.6.11}$$

$$\frac{\partial u'}{\partial x} + \frac{\partial w'}{\partial z} = 0, \tag{7.6.12}$$

$$\frac{\partial b'}{\partial t} + u' f\bar{V}_z + N^2 w' = \kappa\frac{\partial^2 b'}{\partial z^2}, \tag{7.6.13}$$

where ζ_{ga} is the basic state absolute vorticity ($v_{gx} + f$), ν the momentum diffusivity, κ the thermal diffusivity, ρ_o the constant reference density, b' the perturbation buoyancy ($(g/\theta_o)\theta'$), and p' the perturbation pressure. Based on the incompressible continuity equation, (7.6.12), we may assume a streamfunction such that $u' = -\partial\psi/\partial z$ and $w' = \partial\psi/\partial x$. Thus, the above equation set may be written in terms of ψ,

$$D_\kappa D_\nu^2 \frac{\partial^2\psi}{\partial z^2} + D_\nu\left(N^2 \frac{\partial^2\psi}{\partial x^2} - f\overline{V}_z \frac{\partial^2\psi}{\partial x \partial z}\right) + D_\kappa\left(\zeta_{ga} f \frac{\partial^2\psi}{\partial z^2} - f\overline{V}_z \frac{\partial^2\psi}{\partial x\partial z}\right) = 0, \quad (7.6.14)$$

where

$$D_\nu = \frac{\partial}{\partial t} - \nu\frac{\partial^2}{\partial z^2} \text{ and } D_\kappa = \frac{\partial}{\partial t} - \kappa\frac{\partial^2}{\partial z^2}.$$

The above equation may be non-dimensionalized by applying the following scaling,

$$z^* = Hz; \qquad x^* = \left(\frac{HN^2}{f\overline{V}_z}\right)\left(\frac{\sigma}{1+\sigma}\right)x; \qquad t^* = 1/\sqrt{f\overline{\zeta}_a}\, t, \qquad (7.6.15)$$

where $\sigma = \nu/\kappa$ is the Prandtl number and the asterisk denotes a dimensional quantity. Note that the scale of x is determined by the depth of the fluid and the slope of the θ surfaces, as indicated in (7.6.8). Substituting (7.6.15) into (7.6.14) yields (with star symbol dropped)

$$D_\sigma D^2 \frac{\partial^2\psi}{\partial z^2} + \chi D\left(\frac{\partial^2\psi}{\partial x^2} - \frac{\sigma}{1+\sigma}\frac{\partial^2\psi}{\partial x\partial z}\right) + D_\sigma\left(\frac{\partial^2\psi}{\partial z^2} - \frac{\chi}{1+\sigma}\frac{\partial^2\psi}{\partial x\partial z}\right) = 0, \qquad (7.6.16)$$

where

$$D = \frac{\partial}{\partial t} - T^{1/2}\frac{\partial^2}{\partial z^2}; \quad D_\sigma = \sigma\frac{\partial}{\partial t} - T^{1/2}\frac{\partial^2}{\partial z^2};$$

$$T = \frac{\nu^2}{f\zeta_{ga}H^4}; \qquad \chi = \left(\frac{f}{\zeta_{ga}R_i}\right)\frac{(1+\sigma)^2}{\sigma}; \quad R_i = \frac{N^2}{\overline{V}_z^2}. \tag{7.6.17}$$

The boundaries at the top and bottom of the domain are specified as rigid ($w' = 0$) and non-conducting ($b' = 0$). The free-slip boundary condition requires $\partial u'/\partial z = 0$, while the no-slip boundary condition requires $u' = 0$. The boundary conditions in dimensional form may be written as

$$\psi = \frac{\partial^2\psi}{\partial z^2} = \frac{\partial u'}{\partial z} = b' = 0 \qquad \text{for free-slip case;} \tag{7.6.18a}$$

$$\psi = \frac{\partial^2\psi}{\partial z^2} = u' = b' = 0 \qquad \text{for no-slip case.} \tag{7.6.18b}$$

The steady overturning problem may be investigated by setting the time derivative in (7.6.16) equal to 0 and integrating twice in z to obtain

$$T\frac{\partial^6\psi}{\partial z^6} + \chi\frac{\partial^2\psi}{\partial x^2} - \chi\frac{\partial^2\psi}{\partial x\partial z} + \frac{\partial^2\psi}{\partial z^2} = 0. \tag{7.6.19}$$

The constants of integration can be shown to be 0 for both the free-slip and no-slip boundary conditions (Emanuel 1979). Walton (1975) showed that the first term in (7.6.19) uniformly approaches the inviscid limit at $T \to 0$ in spite of the sixth derivative factor. Hence, the inviscid limit can be obtained by setting $T = 0$,

$$\frac{\partial^2\psi}{\partial x^2}-\frac{\partial^2\psi}{\partial x\partial z}+\frac{1}{\chi}\frac{\partial^2\psi}{\partial z^2}=0. \qquad (7.6.20)$$

We take the normal-mode approach by assuming a wave-like solution $\psi(x,z)=\exp[i(kx+mz)]$, where k and m are the horizontal and vertical wave numbers, respectively. Substituting ψ into the above equation yields a quadratic eigenvalue equation for m. Solving for the two roots gives

$$\psi(x,z)=e^{i(kx+m_1z)}\left(Ae^{im_2z}+Be^{-im_2z}\right), \qquad (7.6.21)$$

where $m_1=(k/2)\chi$ and $m_2=(k/2)(\chi^2-4\chi)^{1/2}$. Applying the free-slip boundary condition $\psi=0$ at the boundaries, $z=0,1$ to (7.6.21) leads to $m_2=n\pi$, $n=1,2,3,....$ and a quadratic equation in χ with the physical solution given by

$$\chi=2+2\sqrt{1+(n\pi/k)^2}, \quad n=1,2,3,... \qquad (7.6.22)$$

This means the smallest value for χ is 4, which occurs as $k\to\infty$. Based on the definition of χ in (7.6.17), we have $\chi\propto 1/R_i\propto\overline{V}_z^2$, which gives the maximum or critical Richardson number and minimum vertical wind shear,

$$R_{ic}=\left(\frac{f}{\zeta_{ga}}\right)\frac{(1+\sigma)^2}{4\sigma}, \qquad (7.6.23)$$

$$\overline{V}_{z,\min}=\frac{N}{\sqrt{R_{ic}}}. \qquad (7.6.24)$$

Thus, the most unstable mode of symmetric instability can develop only when the vertical wind shear is stronger than $\overline{V}_{z,\min}$. Since both ν and κ may approach 0 in such a way that the Prandtl number (σ) remains finite, σ therefore appears in R_{ic} in an invscid flow (Emanuel and Raymond 1984). It can be shown that in the strictly inviscid case with $\sigma = 1$, the critical (maximum) Richardson number becomes ζ_{ga}/f. The *geostrophic potential vorticity*, as defined by

$$q_g = \frac{g}{\theta_o}(\boldsymbol{\zeta_a} \cdot \nabla\theta) = \zeta_{ga} N^2 \left(1 - \frac{f}{\zeta_{ga}} \frac{1}{R_i}\right), \qquad (7.6.25)$$

becomes 0 when the Richchardson number becomes critical. Hence symmetric instability occurs when $q_g < 0$, which requires the existence of frictional and diabatic processes.

If one assumes, as in the above analysis, that $\partial/\partial x = 0$ and defines the absolute momentum M as $u - fy$ in the (y, z) plane, then (7.6.19) under the new coordinate system becomes (e.g. Emanuel 1979)

$$T\frac{\partial^6\psi}{\partial z^6} + \chi\frac{\partial^2\psi}{\partial y^2} + \chi\frac{\partial^2\psi}{\partial y\partial z} + \frac{\partial^2\psi}{\partial z^2} = 0, \qquad (7.6.26)$$

Figure 7.12 shows one example of the flow fields solved from the above equation at the onset of dry symmetric instability for a viscous flow with free-slip boundary conditions and $T = 10^{-4}$. The sloped dashed line indicates the orientation of the potential temperature surfaces at $\sigma = 1$. The Ekman layer depth δ defined by the equation $\delta = \sqrt{2\nu/f} = \sqrt{2}HT^{1/4}$ is

depicted in the lower left portion of Fig. 7.12a. The streamlines take the form of an ellipse with the long axis tilted along the isentropic surfaces. The slope of the streamlines is very close to that of the isentropic surfaces. The zonal perturbation velocity (u') is heavily influenced by Coriolis turning of the meridional wind (v') (Fig. 7.12b). Negative correlations of u' and w' are evident in the figure, and substantial temperature advection can be seen near the boundaries (Figs. 7.12c and 7.12a).

Strictly speaking, symmetric instability should be determined by hydrostatically and geostrophically balanced mean states (e.g., Persson and Warner 1995; Xu 1992). In observational studies, the geostrophically balanced basic state wind is often approximated by the total wind and the hydrostatically balanced basic state $\bar{\theta}$ is often approximated by observed θ. In assessing the condition for dry symmetric instability, replacing $\bar{\theta}$ by θ is generally a valid approximation, while replacing $\bar{M}$ by M is a poor approximation (Schultz and Schumacher 1999). Another complicated issue is the *partitioning problem*, that is, the question of partitioning the observed flow fields into basic and perturbation states, i.e.. In practice, the geotrophic wind is directly estimated from the observed total pressure or height field. This value is then subtracted from the total wind to obtain the perturbation wind. This implies that the perturbation pressure caused by the unbalanced part of the flow, such as static (gravitational) convection, symmetric instability, and gravity waves, is negligible. This assumption may not be valid after these perturbations are already present (Schultz and Schumacher 1999). Current symmetric instability theories

are applicable only to two-dimensional perturbations. A three-dimensional perturbation on a symmetrically unstable may not necessarily release the instability (Jones and Thorpe 1992; Gu et al. 1998). In addition, symmetric instability can only occur in the presence of a mean horizontal wind with a vertical wind shear. Thus, symmetric instability may also be regarded as a special form of baroclinic instability. Although both baroclinic instability and symmetric instability may simultaneously occur in the atmosphere, the former requires a horizontal temperature gradient, while the latter requires either or both horizontal and vertical shear in the geostrophic wind (Bluestein 1993).

7.6.2 Moist Symmetric Instability

Observational studies indicate that mesoscale cloud and precipitation bands are commonly associated with the frontal zones of extratropical cyclones (e.g. Hobbs 1978; Houze 1993; Emanuel 1994). Whereas some bands are convective in nature, others occur in the absence of convective instability. Many of these bands are parallel to the mean wind shear vector or mean thermal wind (Elliot and Hovind 1964). In fact, Bennetts and Hoskins (1979) applied the layer theory (Emanuel 1983) to their "*conditional symmetric instability"*, thus should be termed as "*potential symmetric instability*" (Schultz and Schumacher 1999), is responsible for the formation of these mesoscale precipitation bands. In the meantime, Emanuel (1979) demonstrated that circulations resulting from the symmetric instability are fundamentally mesoscale in character. Since

then, numerous observational studies have provided evidence that the presence of *moist* (conditional or potential) *symmetric instability* in large scale storms causes some *slantwise convection* and mesoscale precipitation bands (e.g. Bennetts and Sharp 1982; Bennetts and Ryder 1984; also see review in Schultz and Schumacher 1999).

The addition of moisture and its associated effects, such as latent heat release, considerably complicates the theory of dry symmetric instability. Both parcel theory (Emanuel 1983) and layer theory (e.g. Bennetts and Hoskins 1979; Emanuel 1982) have been applied in order to assess the symmetric instability in a moist atmosphere (i.e. moist symmetric instability). The result will allow us to find the conditional symmetric instability (CSI) and potential symmetric instability (PSI), respectively. As will be discussed later, the necessary conditions for CSI and PSI to occur are $\partial \overline{\theta}_e^* / \partial z\big|_{\overline{M}} < 0$ and $\partial \overline{\theta}_e / \partial z\big|_{\overline{M}} < 0$, respectively. This is an analogous condition to $\partial \overline{\theta}_e^* / \partial z < 0$ and $\partial \overline{\theta}_e / \partial z < 0$ for SI and PI to occur, respectively. Note that the $\overline{M}$ in the criteria of CSI and PSI means "along the $\overline{M}$ surface". CSI and PSI have also been misused in the literature (Schultz and Schumacher 1999), so readers should exercise caution when using these terminologies.

When the moist atmosphere is unstable only to upward displacements with finite amplitude, the resulting motions become largely localized in the vicinity of the convective clouds. Parcel theory may be applied as a first approximation in this situation. Characteristics of parcel theory in a dry atmosphere are described in Sec. 7.3.1. In a moist atmosphere, the

parcel is assumed to ascend following the moist adiabat while the environment remains unperturbed. An important assumption that parcel theory makes is that it ignores the effect of perturbation pressure forces on the parcel. To investigate the parcel dynamics of moist symmetric instability, we consider a meridional, steady, moist baroclinic shear flow in thermal wind balance, as shown in Fig. 7.13. A tube of air extending from positive to negative infinities along y direction is initially at rest at z=0. We assume that the perturbation pressure forces acting on the moving air tube are negligible and that there is no turbulent mixing of the air tube with its environment. We will then examine the stability of this air tube after a finite displacement in an arbitrary direction in the x-z plane. We may define the absolute momentum, $M = v + fx$, which, following the motion of the air tube, is conserved, i.e. $DM/Dt = 0$. (This definition is arrived at through a similar process in determining the absolute momentum for inertial and dry symmetric instability.) The horizontal momentum equation governing the motion of the air tube is identical to (7.5.10),

$$\frac{Du}{Dt} = f(v - v_g) = f\left(M - \overline{M}\right), \tag{7.6.27}$$

while the vertical momentum equation of the air tube is identical to (7.3.5),

$$\frac{Dw}{Dt} = g\left(\frac{\overline{\rho} - \rho}{\rho}\right) = g\left(\frac{\alpha - \overline{\alpha}}{\overline{\alpha}}\right), \tag{7.6.28}$$

where α and $\overline{\alpha}$ are the specific volumes of the air tube and the environment, respectively. Following Emanuel (1994), Eq. (7.6.28) may be expressed in terms of the conserved variables. First, we assume $\alpha - \overline{\alpha}$ is a small perturbation from $\overline{\alpha}$. Then, we recognize it is measured at constant pressure, as assumed in the parcel theory. Since α is a function of pressure, the *entropy* (ϕ), and *total water content* (q_w), $\alpha - \overline{\alpha}$ may be approximated by

$$(\alpha - \overline{\alpha})_p \approx \left(\frac{\partial \alpha}{\partial s}\right)_{p,q_w} (s - \overline{s}) + \left(\frac{\partial \alpha}{\partial q_w}\right)_{p,s} (q_w - \overline{q}_w). \qquad (7.6.29)$$

Again, the overbar denotes quantity of the environment, and the entropy is defined as $ds = dq/T$, where *dq* is the addition of heat to a unit of gas at temperature T. The definition of entropy arises from purely mathematical considerations and is based on the second law of thermodynamics. Derivations show quite simply that entropy is related to the potential temperature, i.e. $ds = c_p d(\ln\theta)$. The dry entropy (s_d) and moist (saturation) entropy (s^*) should be used if the air is unsaturated and saturated, respectively. If we further assume that the change of α due to q_w is negligible, then the above equation is reduced to (Emanuel 1994)

$$(\alpha - \overline{\alpha})_p \approx \left(\frac{\partial \alpha_d}{\partial \phi}\right)_p (s - \overline{s}) \approx \left(\frac{\partial T}{\partial p}\right)_s (s - \overline{s}). \qquad (7.6.30)$$

Substituting (7.6.30) and the hydrostatic equation into (7.6.28) yields an approximation equation for the air tube acceleration,

$$\frac{Dw}{Dt} = \Gamma(s - \bar{s}), \tag{7.6.31}$$

where

$$\Gamma = \begin{cases} -\left(\dfrac{\partial T}{\partial z}\right)_{s_d} = \dfrac{g}{c_p} = \Gamma_d & \text{for unsaturated air tube} \\ -\left(\dfrac{\partial T}{\partial z}\right)_{s*} = \Gamma_s & \text{for saturated air tube} \end{cases} \tag{7.6.32}$$

and

$$s = \begin{cases} c_p \ln\theta & \text{for unsaturated air tube} \\ c_p \ln\theta_e^* & \text{for saturated air tube,} \end{cases} \tag{7.6.33}$$

where θ_e^* is the saturation equivalent potential temperature, as defined earlier. Equation (7.6.32) may also be rewritten in terms of the saturation equivalent potential temperature

$$\frac{Dw}{Dt} = \begin{cases} g \ln\left(\dfrac{\theta}{\bar{\theta}}\right) \approx g\left[\dfrac{\theta - \bar{\theta}}{\bar{\theta}}\right] & \text{for unsaturated air tube} \\ g \ln\left(\dfrac{\theta_e^*}{\bar{\theta}_e^*}\right) \approx g\left[\dfrac{\theta_e^* - \bar{\theta}_e^*}{\bar{\theta}_e^*}\right] & \text{for saturated air tube,} \end{cases} \tag{7.6.34}$$

in which the approximations are valid when the terms inside the square brackets are small.

Therefore, (7.6.27) governs the horizontal displacement of the air tube, while (7.6.31) or (7.6.34) governs the vertical displacement of the air tube. In a moist atmosphere, Eq. (7.6.27) governs the inertial instability, while (7.6.31) or (7.6.34) governs the static instability. Note that (7.6.31) may

lead to several conditions: (a) dry static (gravitational) instability for dry air, (b) conditional instability, or more precisely conditional static (gravitational) instability, for an environment that lifts unsaturated air to saturation, and (c) moist absolute instability for completely saturated air. To demonstrate the process leading to conditional symmetric instability, we consider a hypothetical environment shown in Fig. 7.13, where both $\overline{M}$ and $\bar{s}$ surfaces increase upward and eastward ($+x$ direction). Similar to those in Fig. 7.11b, a tube of air displaced vertically upward acquires a negative value of $s-\bar{s}$ and is then accelerated downward toward the original position, according to (7.6.31). In the meantime, a tube of air displaced horizontally to the right acquires a negative value of $M-\overline{M}$ and is accelerated to the left toward the original position, according to (7.6.27). Notice that the air tube moving along the $\bar{s}$ surface experiences no vertical acceleration since the entropy of the air tube (s) is conserved in the displacement and will always be the same as its environment ($\bar{s}$). The air tube moving along the $\overline{M}$ surface experiences no horizontal acceleration since the absolute momentum of the air tube (M) is conserved in the displacement and will always be the same as its environment ($\overline{M}$). The argument made for dry symmetric instability can be applied similarly here. If the air tube moves upward from point D, staying within the region confined by the $\bar{s}$ and $\overline{M}$ surfaces, and accelerates away from D we say it is symmetrically unstable. On the other hand, an air tube that moves from point O to B upward within the region confined by the $\overline{M}$ and $\bar{s}$ surfaces will decelerate back toward O, i.e., it is

symmetrically stable. As a general rule, when the air tube is displaced an arbitrary distance in some arbitrary direction, it will accelerate vertically toward its $\bar{s}$ surface and horizontally toward its $\overline{M}$ surface. Thus, points O and D are stable equilibria of moist symmetric instability for reversible displacement, while point B is an unstable equilibrium for reversible displacement. Analogous to the conditional instability, an air tube originally located at point A needs to be forced to B in order to become symmetrically unstable. Since the symmetric instability is dependent on the air tube being forced to a point beyond B, the instability is referred to as *conditional symmetric instability*. Points B and D may be called the *level of free convection* (LFC) and the *level of neutral buoyancy* (LNB), respectively, for the conditional symmetric instability, which corresponds to the levels for the conditional instability. In the above analysis, the $\bar{\theta}_e^*$ surface may replace the $\bar{s}$ surface.

To illustrate an air tube's motion and maximum velocities, we consider a simple conditional symmetrically unstable atmosphere with idealized $\bar{\theta}_e^*$ and $\overline{M}$ surfaces, as sketched in Fig. 7.14. Figure 7.14 may be viewed as an idealized configuration of Fig. 7.13 because it assumes that the air tube is saturated and at rest at $(x, z) = (0, 0)$. The basic state of the atmosphere is in thermal wind balance. Above $z = H$, there is no vertical shear, so the $\overline{M}$ surfaces are oriented vertically. The $\bar{\theta}_e^*$ surfaces are oriented vertically (horizontally) below (above) $z = H$. The $\overline{M}$ and $\bar{\theta}_e^*$ surfaces may be described as

$$\overline{M} = v_{gz} z + (v_{gx} + f)x = v_{gz} z + \zeta_{ga} x \,, \tag{7.6.35}$$

where v_{gz} and v_{gx} are the constant, positive vertical and horizontal shears of v_g, respectively, ζ_{ga} the absolute geostrophic vorticity of the environment. It follows that

$$\frac{\partial \overline{M}}{\partial x} = v_{gx} + f \,, \tag{7.6.36}$$

$$\frac{\partial \overline{M}}{\partial z} = v_{gz} = \frac{g}{f\theta^*_{eo}} \frac{\partial \overline{\theta}^*_e}{\partial x} \,, \tag{7.6.37}$$

according to the thermal wind relation of a Boussinesq environmental fluid. Substituting $v_g \approx v_{go} + v_{gx} x + v_{gz} z$, and $v(t) = v_{go} - fx$, which can be obtained by integrating (7.5.11), into (7.6.27) leads to the equation governing the horizontal acceleration,

$$\frac{Du}{Dt} = \frac{D^2 x}{Dt^2} = -f\left[v_{gz} z + (f + v_{gx})x\right]. \tag{7.6.38}$$

The equation governing the vertical acceleration may be obtained by substituting $\overline{\theta}^*_e \approx \overline{\theta}^*_{eo} + (\partial \overline{\theta}^*_e / \partial x)x$ and (7.6.37) into (7.6.34)

$$\frac{Dw}{Dt} = \frac{D^2 z}{Dt^2} = -f v_{gz} x \,, \tag{7.6.39}$$

where we assume $\theta^*_e = \overline{\theta}^*_{eo}$ at the original point. Differentiating (7.6.38) twice with respect to t and substituting from (7.6.39) leads to

$$\frac{D^4x}{Dt^4} + (f\zeta_{ga})\frac{D^2x}{Dt^2} - (fv_{gz})^2 x = 0, \tag{7.6.40}$$

where $\zeta_{ga} = f + v_{gx}$ is the absolute geostrophic vorticity, as defined earlier. To solve Eq. (7.6.40), we use the *method of normal modes*, assuming an arbitrary disturbance may be resolved into independent modes of the form $x = \exp(i\omega t)$. Substituting *x* into (7.6.40) leads to the *eigenvalue relation*,

$$\omega^2 = \left(\frac{f\zeta_{ga}}{2}\right)\left[-1 \pm \sqrt{1 + (2v_{gz}/\zeta_{ga})^2}\right]. \tag{7.6.41}$$

For $fv_{gz} >> \zeta_{ga}$, the right hand side of the above equation may be approximated by $\pm fv_{gz}$, which gives four normal modes,

$$\omega = \pm\sqrt{fv_{gz}}; \quad \pm i\sqrt{fv_{gz}}. \tag{7.6.42}$$

Thus, we may assume a general solution with the following form

$$x = A_1 e^{i\sigma t} + A_2 e^{-i\sigma t} + A_3 e^{-\sigma t} + A_4 e^{\sigma t}, \tag{7.6.43}$$

where $\sigma = \sqrt{fv_{gz}}$ and $A_i's$ are constant coefficients to be determined by the initial conditions. Substituting (7.6.43) into (7.6.40) with four initial conditions

$$x = 0, \;\; z = 0, \;\; u_o = 0, \;\; \text{and } w_o = 0, \tag{7.6.44}$$

and Eq. (7.6.39) yields the solution

$$x = \frac{u_o - w_o}{2\sigma}\sinh(\sigma t) + \frac{u_o + w_o}{2\sigma}\sin(\sigma t), \tag{7.6.45}$$

$$z = \frac{w_o - u_o}{2\sigma}\sinh(\sigma t) + \frac{u_o + w_o}{2\sigma}\sin(\sigma t). \tag{7.6.46}$$

The above solution indicates that the hyperbolic function dominates for large time, causing the air tube to accelerate in a way that $x = -z$. Therefore, the air tube accelerates slantwise at an angle of 45° to the left (-*x* direction) from the vertical. This trajectory lies halfway between the $\overline{M}$ and $\overline{\theta}_e^*$ surfaces. The displacement triggers not only the exponentially growing modes, but also oscillatory motion. The horizontal and vertical velocities may be easily obtained by taking the total derivatives of (7.6.45) and (7.6.46),

$$u = \frac{1}{2}(u_o - w_o)\cosh(\sigma t) + \frac{1}{2}(u_o + w_o)\cos(\sigma t), \tag{7.6.47}$$

$$w = \frac{1}{2}(w_o - u_o)\cosh(\sigma t) + \frac{1}{2}(u_o + w_o)\cos(\sigma t). \tag{7.6.48}$$

For $t >> 1/\sigma$, the hyperbolic function terms in (7.6.45)-(7.6.48) dominate, which gives

$$z = -x; \quad u = \sigma x; \quad w = -\sigma x. \tag{7.6.49}$$

As sketched in Fig. 7.14, when the air tube is pushed upward and to the left, it accelerates in the same direction until it reaches the $\overline{\theta}_e^*$ surface at $z = H$, at which $x = -H$, $u = -\sigma H$ and $w = \sigma H$. After reaching $z = H$, the air tube loses upward acceleration due to the lack of buoyancy. However, it continues to accelerate to the left, but oscillates vertically about the $\overline{\theta}_e^*$

surface until it reaches the $\overline{M}$ surface again. It will then oscillate about the intersection between the $\overline{\theta}_e^*$ surface and the $\overline{M}$ surface. The trajectory of the air tube is denoted in the figure by the solid curve with the arrow.

Analogous to CAPE for conditional instability, a quantity may be defined to calculate the total amount of kinetic energy converted from potential energy available for slantwise free convection. This quantity is known as the *slantwise convective available potential energy* (SCAPE) and is triggered by the conditional symmetric instability associated with the displacement of an air tube. The work per unit mass expended in displacing a tube of air from an initial point *i* to some point *a* in the *x*-*z* plane may be calculated by applying the horizontal and vertical acceleration, i.e. (7.6.27) and (7.6.31), to the definition of work,

$$W = \int_i^a \frac{\boldsymbol{F}}{m} \cdot d\boldsymbol{l} = \int_i^a \frac{d\boldsymbol{V}}{dt} \cdot d\boldsymbol{l} = \int_i^a \left[f(M - \overline{M})\boldsymbol{i} + \Gamma(s - \overline{s})\boldsymbol{k} \right] \cdot d\boldsymbol{l} \,. \qquad (7.6.50)$$

Since the work done in displacing the air tube from *i* to position *a* is independent of the path, we choose to integrate the above equation along the $\overline{M}$ surface,

$$W = \int_i^a \Gamma(s - \overline{s})\,(dz)_{\overline{M}} \,. \qquad (7.6.51)$$

Thus, SCAPE may be defined as the work done in displacing the air tube from its LFC to LNB,

$$SCAPE = \int_{z_{LFC}}^{z_{LNB}} \Gamma(s - \overline{s})\,(dz)_{\overline{M}} \,, \qquad (7.6.52)$$

The above equation may also be written in terms of the specific volume,

$$SCAPE = \int_{z_{LFC}}^{z_{LNB}} g\left(\frac{\alpha - \overline{\alpha}}{\overline{\alpha}}\right)(dz)_{\overline{M}} = -\int_{p_{LFC}}^{p_{LNB}} g(\alpha - \overline{\alpha})(dp)_{\overline{M}} . \qquad (7.6.53)$$

Since the work done in displacing the air tube from its initial point *i* to some point *a* is path independent, however, we may also express (7.6.50) along an $\bar{s}$ surface,

$$SCAPE = \int_{x_{LFC}}^{x_{LNB}} f(M - \overline{M})(dx)_{\bar{s}} , \qquad (7.6.54)$$

or in general as

$$SCAPE = \int_{z_{LFC}}^{z_{LNB}} \Gamma(s - \bar{s})\, dz + \int_{x_{LFC}}^{x_{LNB}} f(M - \overline{M})\, dx . \qquad (7.6.55)$$

If the atmosphere is barotropic, then SCAPE is the same as CAPE since the $\overline{M}$ surfaces are vertical. On the other hand, the *slantwise convective inhibition* (SCIN), the work needed to lift an air tube adiabatically and pseudoadiabatically from its original level to LFC for conditional symmetric instability to occur, may be defined as

$$SCIN = -\int_{z_i}^{z_{LFC}} \Gamma(s - \bar{s})(dz)_{\overline{M}} , \qquad (7.6.56)$$

or equivalent forms of (7.6.54) and (7.6.55).

It can be shown that extending the $\overline{M} - \bar{\theta}$ *relationship* for dry symmetric instability, i.e. $\overline{M}$ surfaces are less steep than $\bar{\theta}$ surfaces or $|\partial z / \partial x|_{\overline{M}} < |\partial z / \partial x|_{\bar{\theta}}$, to three dimensions is equivalent to (e.g. Hoskins 1974)

$$PV_g = g\left(\boldsymbol{\zeta_{ga}} \cdot \nabla\theta\right) < 0, \qquad (7.6.57)$$

where $\boldsymbol{\zeta_{ga}}$ is the three-dimensional geostrophic absolute vorticity vector. In other words, in the absence of dry static instability and inertial instability, negative geostrophic potential vorticity is a necessary condition for dry symmetric instability. Analogously, the three-dimensional form of the $\overline{M} - \overline{\theta}_e^*$ relationship for CSI, i.e. $\overline{M}$ surfaces are less steep than $\overline{\theta}_e^*$ surfaces or $\left|\partial z/\partial x\right|_{\overline{M}} < \left|\partial z/\partial x\right|_{\overline{\theta}_e^*}$, is equivalent to

$$MPV_g^* = g\left(\boldsymbol{\zeta_{ga}} \cdot \nabla\theta_e^*\right) < 0, \qquad (7.6.58)$$

where MPV_g^* is the *saturated geostrophic potential vorticity*, in the absence of conditional and inertial instabilities. Therefore, using the three-dimensional form of MPV_g^* to assess CSI does not require strict adherence to the same assumptions as using the $\overline{M} - \overline{\theta}_e^*$ relationship for cross-sections (Schultz and Schumacher 1999).

Based on the above discussions, the necessary condition for conditional symmetric instability to occur may be summarized as

$$\partial\overline{\theta}_e^*/\partial z\big|_{\overline{M}} < 0, \qquad (7.6.59a)$$

$$\partial\overline{M}/\partial z\big|_{\overline{\theta}_e^*} < 0, \qquad (7.6.59b)$$

$$\Gamma_s\big|_{\overline{M}} < \gamma\big|_{\overline{M}} < \Gamma_d\big|_{\overline{M}}, \qquad (7.6.59c)$$

$$\left|\partial z/\partial x\right|_{\overline{M}} < \left|\partial z/\partial x\right|_{\overline{\theta}_e^*}, \text{ or} \qquad (7.6.59d)$$

$$MPV_g^* = g\left(\boldsymbol{\zeta}_{ga} \cdot \nabla\theta_e^*\right) < 0, \qquad (7.6.59e)$$

provided that the air tube has been lifted above its LFC and conditional and inertial instabilities are absent in its environment. Figure 7.15a shows the surface pressure (hPa) and 1000-500 hPa thickness (dm) at 1200 UTC 16 November 1983 for a cyclone developing case during the New England Winter Storms Experiment. The day before, the cyclone was weaker and in Tennessee. It then moved to New England, and in doing so, developed into a stronger cyclone. The aircraft-observed sounding along the $\overline{M}$ surface was very close to moist-neutral, down to about 650 hPa. However, the vertical sounding indicates the sounding is statically (gravitational) stable (Fig. 7.15b). Thus, the atmosphere appears to prefer slantwise neutrality. The $\overline{M}$ and $\overline{\theta}_e^*$ surfaces constructed from 0000 UTC 16 November soundings and plotted on the cross section from Caribou, Maine (CAR) through Portland, Maine (PWM) to Chatham, Massachusetts (CHH) are shown in Fig. 7.16a. Regions with a lapse rate along $\overline{M}$ surfaces that are greater than or equal to the moist adiabat, i.e. $\Gamma_s|_{\bar{M}} \le \gamma|_{\bar{M}}$, are hatched in the figure. In fact, a large portion of the hatched region follows moist adabatic lapse rates along $\overline{M}$ surfaces. Thus, the atmosphere favors a condition of slantwise convective neutrality. Note that slantwise convective neutrality includes both conditional symmetric neutrality (Fig. 7.16a) and potential symmetric neutrality (Fig. 7.16b). The *potential symmetric instability* (PSI) may be assessed by replacing θ_e^* with θ_e in (7.6.59). The conditions for static (gravitational) instability,

conditional instability, potential instability, inertial instability, symmetric instability, conditional symmetric instability, and potential symmetric instability are summarized in Table 7.1.

It is important to note the difference between conditional symmetric instability and potential symmetric instability, even though both tend to produce slantwise convection when conditions are satisfied (Schultz and Schumacher 1999). For example, Fig. 7.7 shows θ_e^* and θ_e surfaces on a cross section from Dauphin, Manitoba (YDN) to Minneapolis-St. Paul (MSP) forecast by Rapid Update Cycle (RUC) valid at 0000 UTC 3 January 1998. Although the air above the frontal surface is conditionally unstable since $\partial\theta_e^*/\partial z < 0$ (Fig. 7.7a), it is potentially stable since $\partial\theta_e/\partial z > 0$ (Fig. 7.7b). This may happen along the $\overline{M}$ surfaces, i.e. $\partial\overline{\theta}_e^*/\partial z\big|_{\overline{M}} < 0$ and $\partial\overline{\theta}_e/\partial z\big|_{\overline{M}} > 0$, which indicates that CSI may occur, but not PSI. Care should be taken in using and distinguishing between CSI and PSI, which have been misused in some literature (Schultz and Schumacher 1999). Bennetts and Hoskins (1979) and Emanuel (1983) have applied the layer theory to study the PSI, which has been evidenced in many examples in the literature. The wet-bulb potential temperature (θ_w) is also a conserved variable under dry and pseudoadiabatic processes and may be equivalently employed for θ_e in diagnosing PSI. At saturation, the vertical gradient of θ_e, θ_e^* and θ_w are equivalent, therefore, CI and PI, as well as CSI and PSI are equivalent.

In the real atmosphere, CI/PI and CSI/PSI may coexist, creating convective-symmetry instability, which then produces mesoscale convective systems (e.g. Jascourt et al. 1988). Two mechanisms, namely *upscale development* and *downscale development*, have been proposed to explain the convective systems triggered by convective-symmetric instability. For the former mechanism, small-scale moist gravitational (static) convection develops first, followed by mesoscale banded organization of clouds due to the release of symmetric instability as the environment stabilizes gravitationally (Xu 1986). Figure 7.17a shows a conceptual model of this type. The upright updraft released by static (gravitational) instability (CI or PI) is followed by a slantwise convection released by symmetric instability (CSI or PSI), which then produces downdrafts that follow sloping (dry and/or moist) isentropes on descent. On the other hand, a downscale convective-symmetric instability may also occur, as sketched in Fig. 7.17b. A possible example of this type of mechanism is the elevator-escalator conceptual model of a warm-frontal ascent, as shown in Fig. 7.17b. The mesoscale circulation is composed of regions of (1) strong sloping ascent tilted about 45^{o} to the horizontal with a width of about 10 km, i.e. elevator triggered by PI, and (2) weaker regions of gentler slantwise ascent tilted about 10^{o} from the horizontal with a width of about 15 km, i.e. escalator triggered by PSI (Neiman et al. 1993).

7.7 Baroclinic Instabiltity

A baroclinic atmosphere is one in which density depends on both the temperature and pressure. In a baroclinic atmosphere, available potential energy is stored in the mean flow due to the horizontal temperature gradient (on the isobaric surface) and the vertical basic wind shear (via the thermal wind balance). The available potential energy stored in a baroclinic atmosphere is analogous to the potential energy stored in a water system where a divider separates two sides of different temperature. When the divider is lifted, the colder (denser) fluid will flow toward the warmer (less dense) fluid. Similarly, if certain criterion is met, the available potential energy stored in a baroclinic atmosphere will be released and converted into perturbation available potential energy and then into perturbation kinetic energy. The release of perturbation kinetic energy, converted from the available potential energy may cause spontaneous growth of small disturbances. The atmosphere will then be referred to as having *baroclinic instability*. Baroclinic instability is considered to be the major mechanism responsible for midlatitude cyclogenesis. For example, the lee cyclogenesis mechanisms discussed in Chapter 6 are based on either baroclinic instability or baroclinic lee waves. Fronts usually evolve from the westerly basic flow via some manifestation of baroclinic instability, which leads to their association with developing baroclinic disturbances. The most rapid intensification of surface cyclones and anticyclones occurs when the horizontal wavelength falls in the range of 1500 to 3000 km (e.g. Bluestein 1993).

Conversion of the available potential energy into kinetic energy requires that $(\overline{v\theta})U_z > 0$ in average, based on Term 4 of Eq. (7.1.5). That is, the heat flux must be positive (northward) for a forward westerly shear flow ($U_z > 0$). Since the perturbation meridional velocity and perturbation potential temperature are related to perturbation pressure as

$$v = \frac{1}{f\rho_o}\frac{\partial p'}{\partial x}; \quad \theta = \frac{\theta_o}{g\rho_o}\frac{\partial p'}{\partial z}, \tag{7.7.1}$$

one may derive

$$\frac{\partial E_T}{\partial t} \propto \frac{-1}{\rho_o N^2}\int_0^{z_T}\overline{\left[\frac{\partial z}{\partial x}\right]_p\left(\frac{\partial p}{\partial z}\right)^2}U_z dz, \tag{7.7.2}$$

based on Eq. (7.1.5). Thus, converting the available potential energy to perturbation kinetic energy requires an upshear tilt of the constant phase of perturbation pressure, i.e. $[\partial z/\partial x]_p < 0$, in average.

The dynamics of baroclinic instability may be elucidated by the Eady model (1949). By making the following assumptions: (1) quasi-geostrophic approximation, (2) Boussinesq approximation, (3) *f*-plane approximation, (4) constant vertical shear of the basic wind, i.e. $U(z) = U_z z$, where U_z is constant, and (5) rigid upper and lower boundaries at $z = 0$ and *H*, the perturbation potential vorticity equation and thermodynamic energy equation may be derived from Eqs. (6.5.6) and (6.5.9),

$$\left(\frac{\partial}{\partial t}+U\frac{\partial}{\partial x}\right)\left[\nabla^2 p'+\frac{f^2}{N^2}\frac{\partial^2 p'}{\partial z^2}\right]=0, \text{ and} \qquad (7.7.3)$$

$$\left(\frac{\partial}{\partial t}+U\frac{\partial}{\partial x}\right)\frac{\partial p'}{\partial z}-U_z\frac{\partial p'}{\partial x}+\rho_o N^2 w=0 \text{ at } z=0,H, \qquad (7.7.4)$$

where ρ_o is a constant reference density under the Boussinesq approximation. As mentioned in Chapter 6, the term inside the square bracket of (7.7.3) is the perturbation potential vorticity. The above two equations form a closed system as long as w is known at $z=0$ (it is assumed to be 0 at $z=0$ and H). This fluid flow system is called the Eady (1949) model except in the height coordinates, which is similar to that adopted by Smith's (1982) lee cyclogenesis theory except that a rigid upper boundary and a flat lower boundary are used in Eady's model.

To solve the problem, we may apply the normal mode approach by assuming the wave-like solution,

$$p'(x,y,z,t)=P_o(z)\cos(ly)\exp[ik(x-ct)], \qquad (7.7.5)$$

where $P_o(z)$ and c are the wave amplitude and phase speed, respectively, and are complex numbers. Substituting (7.7.5) into (7.7.3) and (7.7.4) yields

$$\frac{\partial^2 P_o}{\partial z^2}-m^2 P_o=0, \qquad (7.7.6)$$

$$\frac{\partial P_o}{\partial z}-\left(\frac{1}{z-c/U_z}\right)P_o=0 \text{ at } z=0,H, \qquad (7.7.7)$$

where $m^2 = (k^2 + l^2)N^2 / f^2$. The general solution of equation (7.7.6) can be written as

$$P_o(z) = A\sinh mz + B\cosh mz, \tag{7.7.8}$$

where A and B are the constant coefficients. Applying the upper and lower boundary conditions, Eq. (7.7.7), to (7.7.8) leads to

$$mcA + U_z B = 0, \tag{7.7.9a}$$

$$[m(H - c/U_z)\cosh mH - \sinh mH]A +$$

$$[m(H - c/U_z)\sinh mH - \cosh mH]B = 0. \tag{7.7.9b}$$

A nontrivial solution requires the determinant of the coefficients of A and B to vanish, which gives

$$c = \frac{U_z H}{2}\left[1 \pm \left(1 - \frac{4\cosh mH}{mH\sinh mH} + \frac{4}{m^2 H^2}\right)^{1/2}\right]. \tag{7.7.10}$$

In general, the phase speed c is a complex number, which can be expressed as $c = c_r + ic_i$. Thus, Eq. (7.7.5) may be written as

$$p'(x, y, z, t) = P_o(z)\cos(ly)\exp[ik(x - c_r t)]\exp(kc_i t). \tag{7.7.11}$$

When $c_i > 0$, disturbances grow exponentially and the flow becomes baroclinically unstable. On the other hand, when $c_i < 0$, disturbances decay exponentially and the flow is baroclinically stable. That is, the condition for baroclinic instability to occur is

$$1-\frac{4\cosh mH}{mH\sinh mH}+\frac{4}{m^2H^2}<0\,. \qquad (7.7.12)$$

The critical value for baroclinic instability to occur may be found by setting the left hand side of Eq. (7.7.12) to 0, which yields (Eady 1949; also see reviews in Gill 1982, Pedlosky 1987 and Holton 2004)

$$\left[\frac{m_cH}{2}-\tanh\left(\frac{m_cH}{2}\right)\right]\left[\frac{m_cH}{2}-\coth\left(\frac{m_cH}{2}\right)\right]=0\,, \qquad (7.7.13)$$

where m_c represents the critical vertical wave number. This may be found by setting the terms of the second square bracket equal to 0, which leads to

$$(k^2+l^2)<(mf/N)^2\approx 5.76/L_R^2\,, \qquad (7.7.14)$$

where $L_R\equiv NH/f$ is the Rossby radius of deformation for a continuously stratified fluid, which has a value of about 1000 *km* for a typical atmosphere with $N=0.01\,s^{-1}$, $H=10\,km$, and $f=10^{-4}s^{-1}$. For waves where $k=l$, the wavelength of maximum growth rate is found to be $L_{\max}=2\sqrt{2}\pi L_R/(Hm_{\max})\cong 5500\,km$, for which kc_i is a maximum. However, in the real atmosphere with nonlinearity and latent heating present, the wavelength of the maximum growth rate may be shorter than that predicted by the Eady model (e.g. Bluestein 1993). Substituting this $m_{\max}$ into Eq. (7.7.8) and representing B with A by using (7.7.9), one may obtain the vertical structure of the most unstable wave, as sketched in Fig.

7.18. Both the constant phases of perturbation pressure and vertical motion tilt upshear (westward) with height, a condition required in the conversion of available potential energy into perturbation kinetic energy, Eq. (7.7.2). The warmest and coldest regions, however, tilt downshear (eastward) with height. At all levels, air moving poleward is generally warmer than air moving equatorward (Fig. 7.18c), which results in a net poleward (positive) heat flux.

The baroclinic instability for a flow on the β plane without an upper boundary has been solved by Charney (1947) and is often referred to as *Charney's model* (e.g. Pedlosky 1987). Available potential energy stored in a horizontally sheared basic flow may be released through the *barotropic instability* (e.g. Pedlosky 1987), which has much less impact on mesoscale flow, and thus is not discussed.

Table 7.1: Conditions for different types of instabilities

	Static (Gravitational)	Inertial	Symmetric
Dry	Absolute Instability	Inertial Instability	Symmetric Instability
	$\partial\overline{\theta}/\partial z<0$; $\gamma>\Gamma_d$	$\partial\overline{M}/\partial x<0$; $\zeta_{ga}+f<0$	$\left(\partial\overline{\theta}/\partial z\right)_{\overline{M}}<0$; $\left(\partial\overline{M}/\partial x\right)_{\overline{\theta}}<0$ $\Gamma_d\big\vert_{\overline{M}}<\gamma\big\vert_{\overline{M}}$ $\left\vert\partial z/\partial x\right\vert_{\overline{M}}<\left\vert\partial z/\partial x\right\vert_{\overline{\theta}}$ $PV_g<0$
Moist	Moist Absolute Instability	N/A	N/A
	$\Gamma_s<\gamma_s$		
Conditional[#]	Conditional Instability (CI)	N/A	Conditional Symmetric Instability (CSI)
	$\partial\overline{\theta}_e^*/\partial z<0$ $\Gamma_s<\gamma<\Gamma_d$ (parcel lifted above LFC)		$\partial\overline{\theta}_e^*/\partial z\big\vert_{\overline{M}}<0$; $\partial\overline{M}/\partial z\big\vert_{\overline{\theta}_e^*}<0$ $\Gamma_s\big\vert_{\overline{M}}<\gamma\big\vert_{\overline{M}}<\Gamma_d\big\vert_{\overline{M}}$ $\left\vert\partial z/\partial x\right\vert_{\overline{M}}<\left\vert\partial z/\partial x\right\vert_{\overline{\theta}_e^*}$ $MPV_g^*<0$ (parcel lifted above LFC)
Potential[##]	Potential Instability (PI)	N/A	Potential Symmetric Instability (PSI)
	$\partial\overline{\theta}_e/\partial z<0$		$\partial\overline{\theta}_e/\partial z\big\vert_{\overline{M}}<0$; $\partial\overline{M}/\partial z\big\vert_{\overline{\theta}_e}<0$ $\left\vert\partial z/\partial x\right\vert_{\overline{M}}<\left\vert\partial z/\partial x\right\vert_{\overline{\theta}_e}$

			$MPV_g < 0$

[#]at saturation, $\overline{\theta}_e = \overline{\theta}_e^*$; ## $\overline{\theta}_w$ can be used equivalently for $\overline{\theta}_e$. Meanings of the symbols: (1) γ: observed environmental lapse rate; (2) Γ_d: dry lapse rate; (3) Γ_s: moist lapse rate; (4) γ_s: observed environmental saturated lapse rate; (5) $\overline{\theta}$: environmental potential temperature; (6) $\overline{\theta}_e$: environmental equivalent potential temperature; (7) $\overline{\theta}_e^*$: environmental saturation equivalent potential temperature; (8) $\overline{M}$: environmental geostrophic absolute momentum; (9) PV_g: geostrophic potential vorticity (PV); (10) MPV_g: geostrophic PV; and (11) MPV_g^*: saturated geostrophic potential vorticity.

Figure Captions

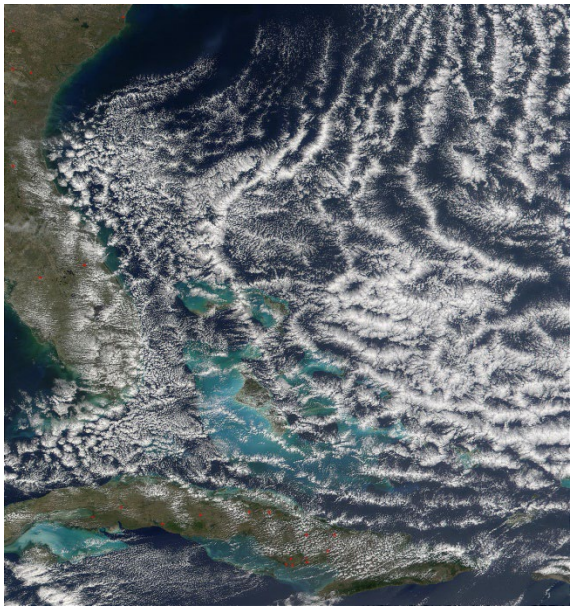

Fig. 7.1: Open cell cloud formation observed over the Atlantic Ocean off the southeast coast of the United States on February 19, 2002, as viewed by satellite Terra. This type of clouds is an atmospheric manifestation of Rayleigh- Be′nard convection is known as mesoscale cellular convection. It normally forms as the cold air passes over the warmer ocean waters. Notice the hexagonal open cells produced in the cloud-topped boundary layer and the convective clouds at the vertices of the hexagonal cells. (From Visible Earth, NASA)

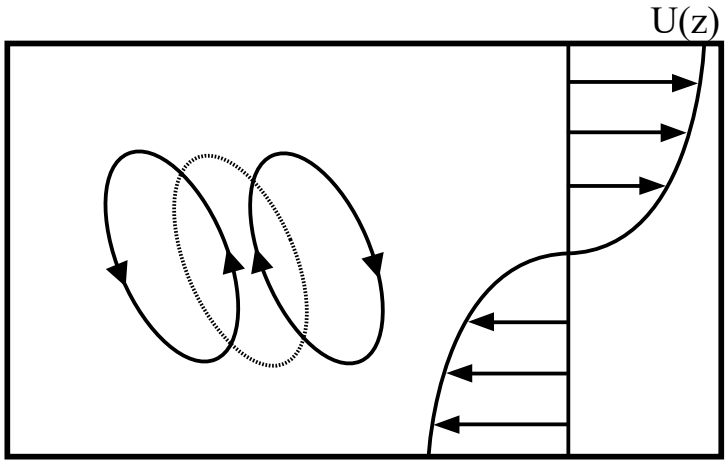

Fig. 7.2: A sketch of the basic wind profile and the upshear tilt of the perturbation streamfunctions (solid) and updraft (dashed) associated with an unstable growing gravity wave in a stably stratified flow. The perturbation wave energy is converted from the basic flow shear. (From Lin and Chun, 1993)

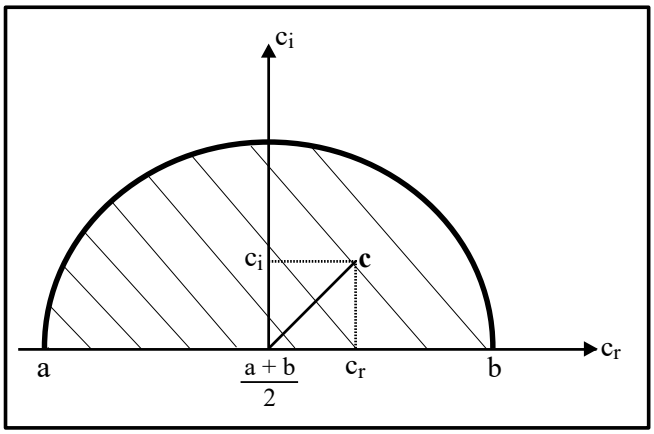

Fig. 7.3: A sketch of the Howard's semicircle theorem.

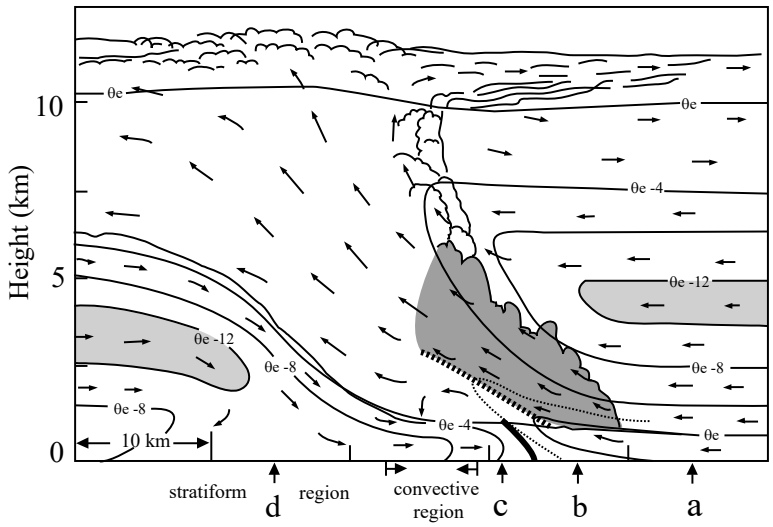

Fig. 7.4: A schematic of the formation of a MAUL through slab convective overturning. Wind vectors relative to the outflow boundary are denoted by arrows, cloud boundaries are denoted by scalloped lines, θ_e contours (every 4 K) are denoted by solid lines, the outflow boundary or frontal zone is denoted by heavy solid line, midlevel layer of low θ_e is highlighted by light shading, and the MAUL is depicted by dark shading. (From Bryan and Fritsch 2000)

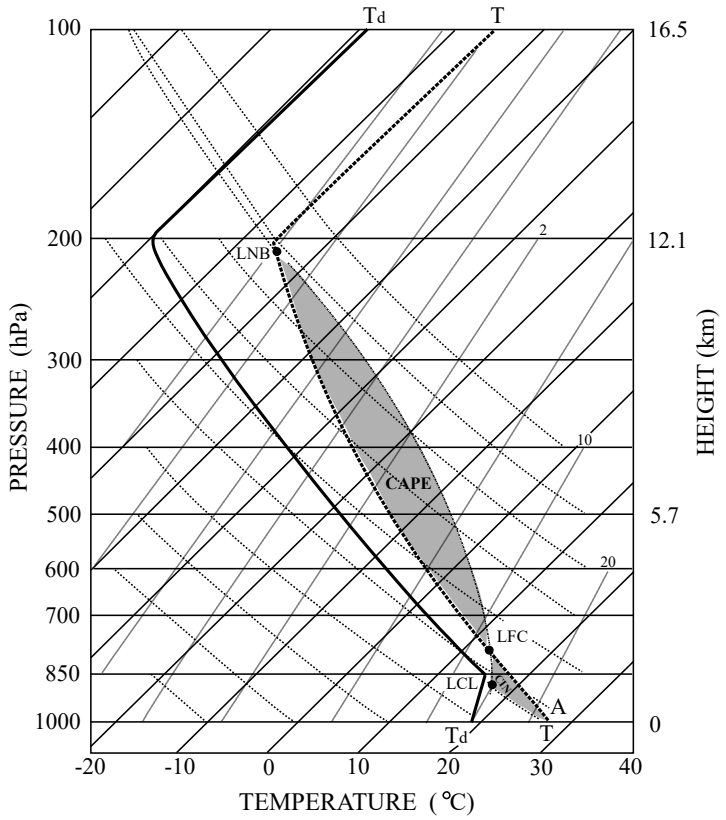

Fig. 7.5: Example of a sounding with conditional instability displayed on a *skew-T log-p* thermodynamic diagram. The lifting condensation level (LCL), level of free convection (LFC), and level of neutral buoyancy (LNB) for the air parcel originated at A are denoted in the figure. The convective available potential energy (CAPE) is the area enclosed by the temperature curve (thick dashed line) and moist adiabat (dot-dashed curve) in between LFC and LNB, while the convective inhibition is the area enclosed the temperature curve and dry adiabat (below LCL) and moist adiabat (above LCL) in between the surface and the LFC.

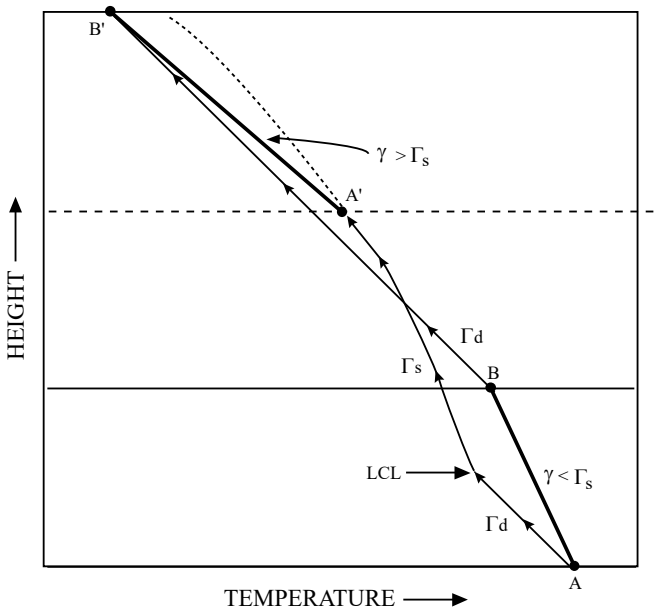

Fig. 7.6: Illustration of potential (convective) instability by lifting an initially absolute stable layer AB with $\partial \overline{\theta}_e / \partial z < 0$. The top of the layer (B) follows a dry adiabat to saturation at B', while the bottom of the layer becomes saturated earlier and then follows moist adiabat to A'. The lapse rate of the final saturated layer (A'B') is greater than the moist adiabat, thus is unstable. (Adapted after Darkow 1986)

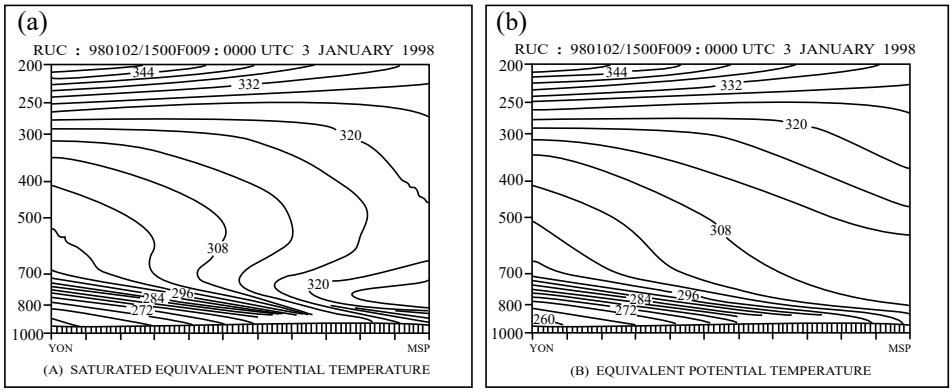

Fig. 7.7: (a) Saturation equivalent potential temperature ($\overline{\theta}_e^*$) and (b) equivalent potential temperature ($\overline{\theta}_e$) fields on the cross section from Dauphin, Manitoba (YDN) to Minneapolis-St. Paul, Minnesota (MSP), as predicted by the Rapid Update Cycle for 9-h forecast valid for 0000 UTC 3 January 1998. Note that above the surface cold front, the air is conditionally unstable ($\partial \overline{\theta}_e^* / \partial z < 0$), but is potentially stable ($\partial \overline{\theta}_e / \partial z > 0$). (Adapted after Schultz and Schumacher 1999)

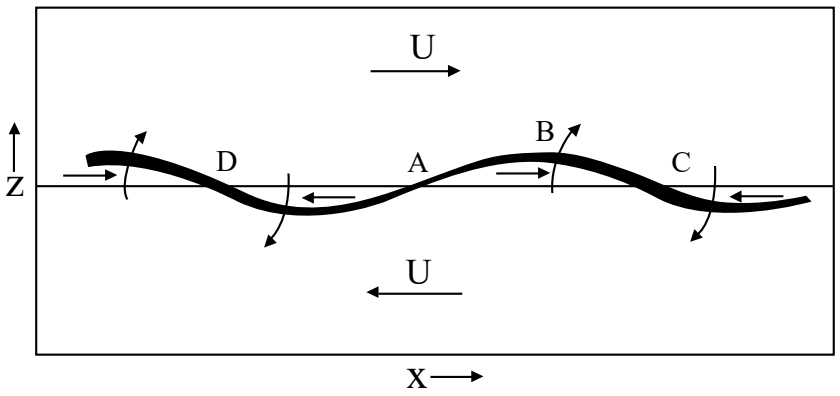

Fig. 7.8: A sketch illustrates the growth of a sinusoidal disturbance to an initially uniform vortex sheet (dashed) with positive vorticity normal to the paper. The local strength of the vortex sheet is represented by the thickness of the sheet. The curved arrows indicate the direction of the self-induced movement of the vorticity in the sheet, and show (a) the accumulation of vorticity at points like *A* and (b) the general rotation about points like *A*, which together lead to exponential growth of the disturbance. (Adapted after Batchelor 1967 and Drazin and Reid 1981)

Fig. 7.9: An example of breaking Kelvin-Helmholtz waves in clouds (billow clouds) formed over Laramie, Wyoming, USA. (Photo by Brooks Martner, NOAA Environmental Technology Laboratory)

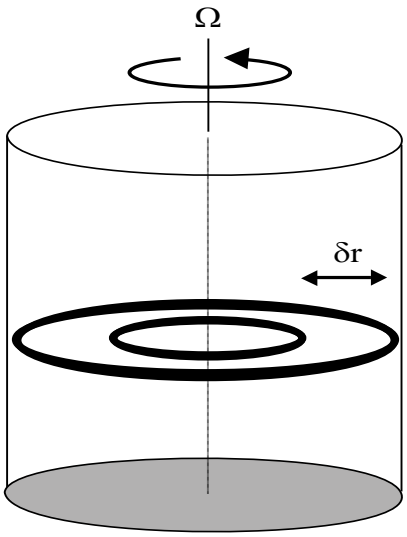

Fig. 7.10: Schematic representation of an inertially stable system of fluid confined by a rotating cylinder. The square of environmental angular momentum ($\overline{M} \equiv u_\theta r = \Omega r$) is assumed to increase with radius. (Adapted after Emanuel 1994)

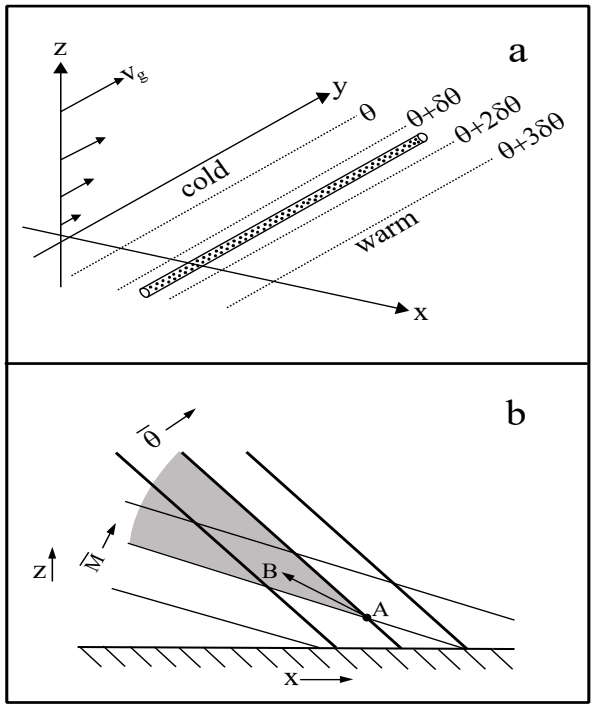

Fig. 7.11: A schematic of a mean state with symmetric instability. (a) A meridional, steady baroclinic flow. The unidirectional geostrophic wind v_g is in thermal wind balance. One may imagine an idealized broad front is aligned with y-axis and located in between the cold and warm region. Under this situation, v_g is the along-front wind. (b) The $\overline{M}$ and $\overline{\theta}$ surfaces on the *x*-*z* plane are tilted such that both of them increase upward and eastward. Displacement of an air parcel upward anywhere within the shaded area from point A is symmetrically unstable (Adapted after Houze 1993).

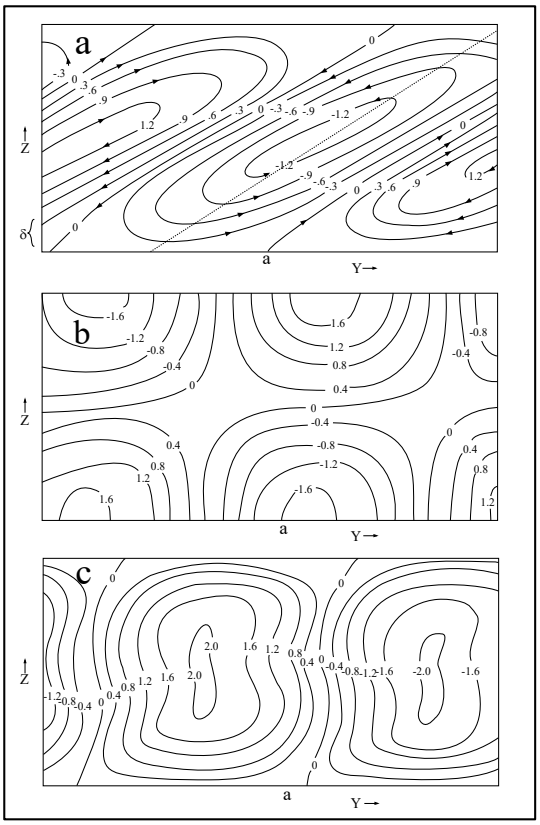

Fig. 7.12: Flow fields solved from Eq. (7.6.26) at the onset of dry symmetric instability for a viscous flow with free-slip boundary conditions and $T = 10^{-4}$. (a) Streamfunction. Dashed line denotes relative orientation of potential temperature surfaces with $\sigma = 1$, and δ at the lower left corner denotes the Ekman (boundary) layer depth. (b) normalized zonal perturbation velocity (u'). Positive values denote flow out of the page. (c) Normalized potential temperature. (From Emanuel 1979)

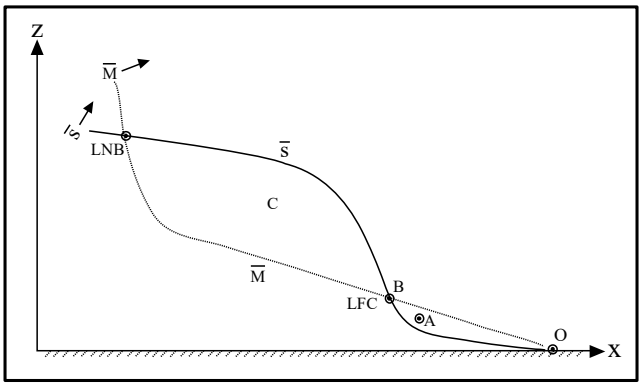

Fig. 7.13: A hypothetical environment for conditional symmetric instability. Distributions of $\overline{M}$ (dashed curve) and $\overline{s}$ (neutral-buoyancy, solid line) surfaces for a tube of air located at the lower right. Domain is approximately 100 km x 10 km. The mean vertical shear vector is pointing into the paper. (Adapted after Emanuel 1983)

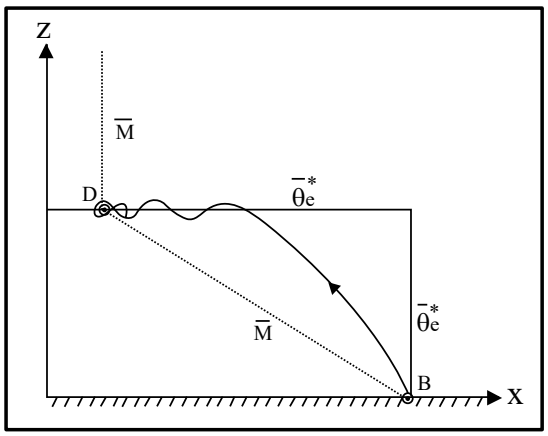

Fig. 7.14: Idealized configuration of $\overline{\theta}_e^*$ (solid line) and $\overline{M}$ (dashed line) surfaces on the *x*-*z* plane for a tube of air in a simple conditional symmetrically unstable atmosphere. The basic state of the atmosphere is in thermal wind balance. Above $z = H$, the basic state flow is barotropic (no shear), thus the $\overline{M}$ surfaces are oriented vertically. The $\overline{\theta}_e^*$ surfaces are oriented vertically (horizontally) below (above) $z = H$. When the air tube is pushed upward and to the left, it accelerates in the same direction until it reaches the $\overline{\theta}_e^*$ surface; it continues to accelerate to the left, but oscillates about the $\overline{\theta}_e^*$ surface at $z = H$ until it reaches the $\overline{M}$ surface again. It will then oscillate about this intersection of $\overline{\theta}_e^*$ surface and $\overline{M}$ surface. The trajectory of the air tube is denoted by the solid curve with arrow. (Adapted after Bluestein 1993 and Emanuel 1983)

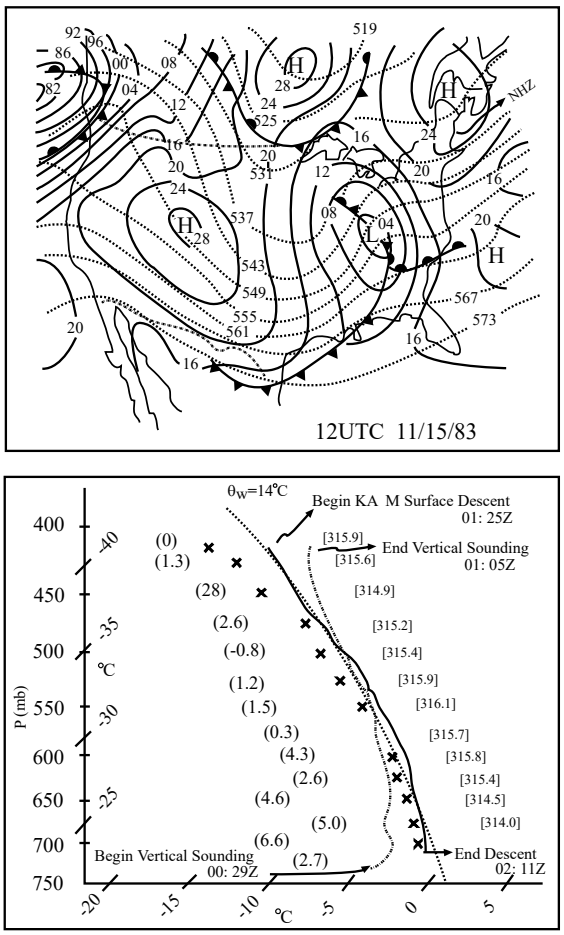

Fig. 7.15: (a) Surface pressure (in hPa) and 1000-500 hPa thickness (dm) at 1200 UTC 16 November 1983. The bar centered at Brunswick, Maine (NHZ) denotes the horizontal projection of $\overline{M}$ surface sounding. (b) $\overline{M}$ surface sounding by aircraft between 0125 and 0211 UTC 16 November 1983. Temperatures and dew points are denoted by solid line and x's, respectively. Numbers to the left indicate departures of $\overline{M}$ (ms^{-1}) from initial value, while numbers to the right indicate θ_e with respect to ice. Dash-dot lineis the temperature sounding made by rapid ascent of aircraft near Brunswick, Maine between 0029 and 0105 UTC 16 November 1983. (After Emanuel 1988)

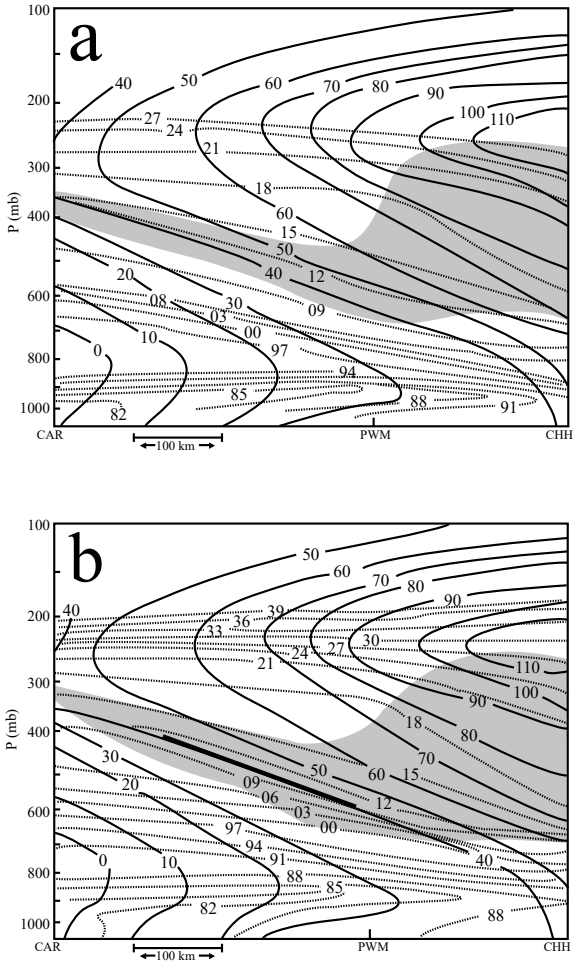

Fig. 7.16: (a) $\overline{M}$ (solid; ms^{-1}) and $\overline{\theta}_e^*$ (dashed; K, with first digit omitted) surfaces on the cross section from Caribou, Maine (CAR) through Portland, Maine (PWM) to Chatham, Massachusetts (CHH) constructed from rawinsonde observations at 0000 UTC 16 November 1983. Region with $\Gamma_m\big|_{\overline{M}} \le \Gamma\big|_{\overline{M}}$ is shaded, within which large portion is moist adiabatic along $\overline{M}$ surfaces. Heavy bar between 400 hPa and 600 hPa denotes partial path of the $\overline{M}$ surface aircraft sounding. (b) Same as (a) except for θ_e, instead of $\overline{\theta}_e^*$. Heavy bar descending through 500 hPa between CR and PWM shows partial path of $\overline{M}$ surface aircraft sounding. (After Emanuel 1988)

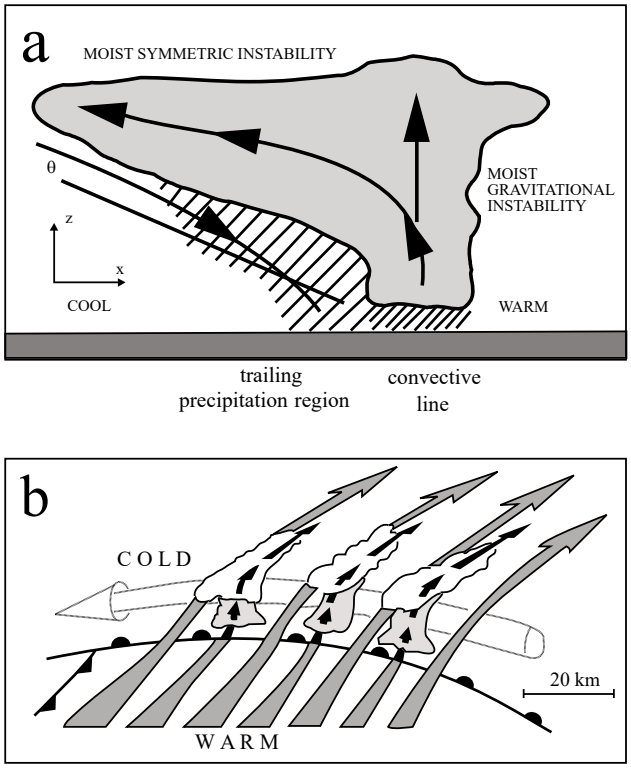

Fig. 7.17: (a) A conceptual model of an upscale convective-symmetric instability in a midlatitude mesoscale convective system. Bold curve encloses cloud (shaded). Thin lines with arrows represent direction of circulation. Grey solid line labeled represents orientation of typical potential-temperature contour in the cool air. Hatching area is proportional to precipitation intensity. The upright updraft released by static (gravitational) instability (CI or PI) is followed by slantwise convection released by symmetric instability (CSI or PSI), which then produce downdrafts that descend following sloping (dry and/or moist) isentropes. (Adapted after Seman 1992 and Schultz and Schumacher 1999) (b) Conceptual model of elevator-escalator of warm-frontal ascent. The mesoscale circulation is composed by regions of (1) strong sloping ascent tilted about 45^{o} to the horizontal with a width of about 10 km, i.e. elevator triggered by PI, and (2) weaker regions of gentler slantwise ascent tilted about 10^{o} from the horizontal with a width of about 15 km, i.e. escalator triggered by PSI. (Adapted after Neiman et al. 1993)

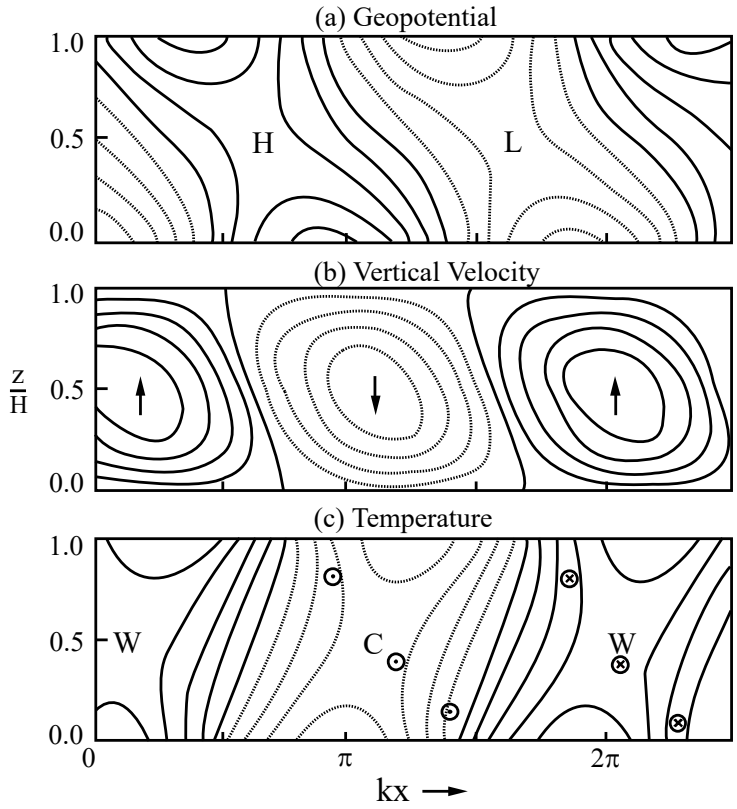

Fig. 7.18: A sketch of vertical structures of the most unstable Eady wave. (a) Perturbation pressure; *H* and *L* denote high and low pressures, respectively. (b) Vertical velocity; up and down arrows denote maximum upward and downward motion, respectively. (c) Perturbation potential temperature; *W* and *C* denote warmest and coldest regions, respectively. Northward and southward meridional velocities are denoted by circles with cross and dot, respectively. (Adapted after Holton 2004)

Problems

1. Derive the energy transfer equation, Eq. (7.1.2) for the fluid system of Eq. (7.1.1) with no north-south (meridional) basic state wind component ($V = 0$), but includes the meridionally sheared zonal flow ($U_y \neq 0$).
2. Derive Eq. (7.2.11).
3. Derive Eq. (7.2.14).
4. Derive Eq. (7.2.29).
5. Derive Eq. (7.2.35)

(Key:

$$0 \geq \int (U-a)(U-b)Rdz = \int U^2 Rdz - (a+b)\int URdz + ab\int Rdz$$

$$= \left[c_r^2 + c_i^2 - (a+b)c_r + ab\right]\int Rdz + \int N^2 |\hat{\eta}|^2 dz$$

$$= \left\{\left[c_r - \frac{1}{2}(a+b)\right]^2 + c_i^2 - \left[\frac{1}{2}(a-b)\right]^2\right\}\int Rdz + \int N^2|\hat{\eta}|^2 dz \,)$$

6. Based on the Poisson equation, Eq. (7.3.1), derive Eq. (7.3.2).
7. Show that the buoyancy force, $g[(\overline{\rho} - \rho)/\rho]$ may be approximated by $g[(\overline{\theta} - \theta)/\theta]$.
8. Consider a fluid system controlled by Eq. (7.3.6), do the following.

   (a) Assuming $N = 0.01\, s^{-1}$, find the vertical displacement of the air parcel (δz) after 10 minutes if the initial vertical displacement of the air parcel is 0 m and vertical velocity is 1 ms^{-1}.

   (b) Find the vertical displacement of an air parcel after 2 minutes for an atmosphere with $N^2 = -10^{-6}\, s^{-2}$, assuming $\delta z = 5\, m$ and $w = 2\, ms^{-1}$ at $t = 0$ s.

   (c) Sketch the vertical displacement of the air parcel versus time and discuss the properties of the parcel motion in (a) and (b).
9. Derive Eq. (7.3.19). (key: (2.68)-(2.70) in Wallace and Hobbs' textbook)
10. Prove that the positive area (PA) defined in Eq. (7.3.21) (the third equality) is equivalent to the CAPE defined in Eq. (7.3.20).
11. Sketch a pair of soundings to show that a layer that is conditionally unstable need not be potentially unstable; nor is a potentially unstable layer necessarily conditionally unstable.
12. Based on Eq. (7.5.8), show that a Rankine vortex is inertially stable for $r \leq r_{\max}$ and inertially neutral for $r > r_{\max}$ for solid body rotation of a homogeneous, inviscid fluid. The Rankine vortex is defined as $V = ar$, where a is a constant, for $r \leq r_{\max}$; $V = b/r$ for $r > r_{\max}$.

13. Substitute $u = Dr/Dt$ into the left side of (7.5.7) and evaluate it at $r = r_o + \delta r$ to derive the governing equation for inertial instability for circular vortex motion. Discuss the three general solutions of the governing equation.
14. Prove the necessary condition for symmetric instability from (7.6.4),

$$\frac{R_i}{f}\left(\frac{\partial v_g}{\partial x} + f\right) < 1 \qquad (7.6.5)$$

15. Following the derivation of Eq. (7.5.14) for inertial instability, derive Eq. (7.6.6) for symmetric instability. (Hint: You may need to approximate v_g by $v_{go} + (\partial v_g/\partial z)_o \delta z + (\partial v_g/\partial x)_o \delta x$ and use $d\overline{\theta} = 0 = (\partial\overline{\theta}/\partial x)\delta x + (\partial\overline{\theta}/\partial z)\delta z$ for displacement along constant $\overline{\theta}$ surface.
16. Based on (7.6.21) and (7.6.22), show that

$$\psi(x,z) = \sin(n\pi z)\sin k\left\{x + \left(1 + \sqrt{1 + (n\pi/k)^2}\ \right)z\right\}, \quad n = 1, 2, 3...$$

is a solution of the streamfunction for steady overturning in an inviscid flow. Plot or make a sketch of the solution by assuming some reasonable flow parameters.
17. Derive Eq. (7.6.40) from Eqs. (7.6.27), (7.5.11), and (7.6.34).
18. Solve the sample problem Eq. (7.6.40) for conditional symmetric instability with the general solution (7.6.43) and initial conditions, i.e. Eq. (7.6.44), and the relation between x and z, (7.6.39) to obtain the solution, Eqs. (7.6.45) and (7.6.46).
19. Derive Eq. (7.7.2).